WATER RESOURCES RESEARCH, VOL. 30, NO. 7, PAGES 2261–2285, JULY 1994

A detachment-limited model of drainage basin evolution

Alan D. Howard

Department of Environmental Sciences, University of Virginia, Charlottesville

Abstract. A drainage basin simulation model introduced here incorporates creep and threshold slumping and both detachment- and transport-limited fluvial processes. Fluvial erosion of natural slopes and headwater channels is argued to be dominantly detachment-limited. Such slopes undergo nearly parallel retreat and replacement with alluvial surfaces under fixed base level, in contrast with gradual slope decline for transport-limited conditions. The arrangement of divides and valleys is sensitive to initial conditions, although average morphology is insensitive. Dissected, initially flat surfaces in which downstream concavity is slight exhibit nearly parallel drainage, compared to very wandering main valleys when concavity is great. Steady state is reached after a cumulative base level drop approximately 3 times the final relief. Simulated valley systems are similar to those predicted by a previous model of optimal drainage basins. A critical value of slope divergence normalized by average slope gradient is a useful criterion for defining the valley network.

Introduction

The advent of high-speed computing permits simulation of the temporal evolution of geomorphic systems, including entire drainage basins. The model introduced here explores general questions of drainage basin evolution, including the following. (1) What is the simplest mathematical model that simulates morphologically realistic landscapes? (2) What are the effects of initial conditions and inheritance on basin form and evolution? (3) What are the relative roles of deterministic and random processes in basin evolution? (4) Do process and form in drainage basins embody principles of optimization? (5) Is there a characteristic drainage basin form that is invariant under waxing or waning relief? (6) What is a practical operational criterion for defining the valley network?

The development of drainage basins, that is, landforms with convex to linear slopes and a dendritic valley network, requires (at a minimum) two superimposed processes. One must be "diffusional" or "dispersive," that is, capable of eroding the land surface with finite gradient for vanishingly small contributing area, but it should become less efficient as contributing area increases, so that gradient increases downslope if rates of surface lowering are locally uniform. The other is a "concentrative" or "advective" process that increases in efficiency with contributing area, but requires large gradients for very small contributing areas. This combination of processes and the spatial transition from creep diffusion on slopes to concentrative runoff processes in channels was recognized very early by *Davis* [1892] and was summarized succinctly by *Gilbert* [1909, pp. 346–347]: "On the upper slopes, where water currents are weak, soil creep dominates and the profiles are convex. On lower slopes water flow dominates and profiles are concave."

As was discussed by *Carson and Kirkby* [1972], *Kirkby* [1971], *Smith and Bretherton* [1972], and numerous subsequent workers, the transport capacity Q of many geomorphic processes can be approximated as a power function of contributing area A and land surface gradient S:

$$Q = K_q A^{\alpha} S^{\beta}, \tag{1}$$

where for most processes $\alpha, \beta \geq 0$. The handover between diffusional and concentrative processes is illustrated by a steady state landscape in which the erosion rate is areally uniform and balances the rate of tectonic uplift U. Then the transport through any location on the landscape must equal, over the long run, the product of uplift rate and contributing drainage area [*Kirkby*, 1980; *Willgoose et al.*, 1991d, 1992; *Tarboton et al.*, 1992]:

$$Q = UA. \tag{2}$$

If the land surface is everywhere "transport-limited," so that actual transport rates equal those given in (1), then [*Willgoose et al.*, 1991d; *Tarboton et al.*, 1992]

$$S = [U/K_q]^{1/\beta} A^{(1-\alpha)/\beta}. \tag{3}$$

Process with $\alpha < 1$ will be diffusional, and those with $\alpha > 1$ will be concentrative. Mass-wasting processes are usually diffusional, and creep is commonly modeled with $\alpha = 0$ and $\beta = 1$. Transport of sand in alluvial channels is concentrative with $\alpha \simeq 1.5$ and $\beta \simeq 2$. Drainage basins will result from a linear combination of a diffusional and concentrative process, with the handover between the processes occurring at that contributing area where they have equal required gradients, thus determining the drainage density and the basin scale. *Smith and Bretherton* [1972], *Kirkby* [1980], *Loewenherz* [1991], and *Tarboton et al.* [1992] discuss basin development and landscape scale for transport-limited processes in a general framework not restricted to steady state landscapes.

In many, perhaps most, landscapes the actual transport rates are in some places considerably less than would be predicted for transport-limited processes. One case occurs when bedrock is exposed on slopes and the rate of local erosion is determined by weathering rates ("weathering-limited" conditions [*Carson and Kirkby*, 1972]). The volume

Paper number 94WR00757.
0043-1397/94/94WR-00757$05.00

of bed sediment transport by wash processes on hillslopes and low-order rills and channels is argued below to be limited by the ability of the flow to entrain or erode regolith (residual soils or colluvium) or bedrock, giving "detachment-limited" conditions [*Howard*, 1994]. The rate of detachment can be quantified in much the same way as the potential rate of transport. The combination of transport-limited mass wasting with detachment-limited wash processes also produces drainage basins, because at steady state the gradient of detachment-limited channels follows a relationship similar to (3). However, the transient response of detachment-limited landscapes to variations in rate of uplift (or base level lowering) is considerably different than for transport-limited conditions, with important implications for landscape evolution. The landform model of *Ahnert* [1976, 1977, 1987a] also distinguishes between suspended-load (detachment limited) and point-to-point (transport limited) runoff erosion.

Few systematic observations have been made of transport and erosion by water in natural headwater slopes and channels. The following observations in support of detachment-limited conditions are based upon the author's informal observations of slopes in the United States in areas of moderate to high relief in areas of humid temperate, mediterranean, and arid climates. Erosion by overland flow and ephemeral rilling on steep, vegetated slopes is nearly always detachment limited owing to the protection offered by the leaves, stems, and roots. Ephemeral or perennial rills on such slopes usually lack a loose sedimentary cover, with exposure of cohesive regolith or rock pavements where flow has removed vegetation. As is discussed by *Howard* [1994], rills and steep washes on badland slopes are generally also detachment-limited owing to the shale or regolith cohesion. Slopes with transport-limited conditions in overland flow and headwater rills seem to be confined to bare, low-gradient slopes with fine-grained, friable regolith, as may occur on some agricultural slopes in sandy soils, dissected alluvial deposits, and the low-relief, sandy slopes discussed by *Dunne and Dietrich* [1980] and *Dunne and Aubrey* [1986]. The absence of an alluvial cover on the slope or in ephemeral rills under low- or no-flow conditions is diagnostic of detachment-limited conditions.

Diffusional process are commonly equated with mass wasting and concentrative processes with wash processes, but common exceptions occur. *Gilbert* [1909], *Howard* [1970], *Moseley* [1973], *Dunne* [1980], and *Dunne and Aubrey* [1986] have noted that rain splash is a diffusive process that can create convex divides and inhibit rilling. In circumstances where stream discharge decreases downstream or where transport of coarse bed load in stream networks occurs without downstream fining, the exponent α may be less than unity, producing a diffusional regime. In fact, diffusion equations are commonly used to model sediment basin deposition [*Flemings and Jordan*, 1989; *Paola*, 1989; *Paola et al.*, 1992; *Rivenaes*, 1992]. Snow and rock avalanches on steep, bedrock slopes can produce concentrative erosion, eroding chutes to create spur and gully terrain [*Matthes*, 1938; *Blackwelder*, 1942; *Rapp*, 1960a, b; *Howard*, 1990b; *Howard and Selby*, 1994]. The debris flows and avalanches frequently originating from colluvial hollows in high-relief, vegetated, soil-mantled slopes are an important erosional agent along the steep, low-order channels through which the flows move [*Hack and Goodlett*, 1960; *Williams and Guy*, 1973; *Osterkamp and Costa*, 1986; *Dietrich and Dunne*, 1978; *Benda*, 1990; *Seidl and Dietrich*, 1992; *Kirkby*, 1987]. The requirements for a critical volume of surface or regolith water, a sufficiently steep slope, an accumulation of colluvium in hollows, and the flowlike behavior after mobilization lead to such avalanches being concentrative processes.

Several quantitative models of landform development have been published over the last 20 years. The pioneering efforts of *Kirkby* [1971, 1976a, b, 1985a, b, 1989] and of *Ahnert* [1976, 1977, 1987a, b, 1988] have helped to define the appropriate process laws and explore their implications for drainage basin form, although most of these studies have been limited to analytical solutions under restricted process and boundary conditions or simulations of slopes only in profile. Numerous other studies have focused on the factors controlling stream morphology, longitudinal stream profile evolution, and drainage network development.

Although a few simulations have been made of erosional processes and drainage network development on slopes [*Armstrong*, 1976; *Kirkby*, 1985b, 1986; *Dunne and Aubry*, 1986], the model of *Willgoose et al.* [1991a, b, c] and its descendants are the only attempts at high-resolution, process-based simulation modeling of slope and channel development at the basin scale. The present model contrasts with that of *Willgoose et al.* [1991a, b, c] in major respects. The Willgoose model (along with most previous models) assumes that overland flow as well as flow in channels is transport limited, whereas the present model assumes that erosion in many locations, particularly in headwaters, is detachment-limited.

The Willgoose model also assumes that individual simulation cells are either channels or slopes, with a "channel activation" function determining transitions between node types. In the present model there is no such distinction, with both fluvial and slope processes assumed to occur within each cell. This leads to a simpler set of governing equations. The use of an activation function in the Willgoose model automatically defines the channel network and drainage density. In the present model the location of channel heads is defined by a morphometric criterion.

The Model

General Features and Assumptions

Within each square matrix cell of dimension δ by δ both slope and channel processes occur. The width W of the active channel is specified to be less than δ, even for alluvial pediments and alluvial fans, corresponding to the observation that flow on such surfaces is generally channelized and confined to a few active channels at any time. Both mass wasting and fluvial transport/erosion occur in each cell.

Downstream within the drainage basin the channels dominate the processes within each cell. However, close to divides, erosion by mass wasting is commensurate with, or greater than, channel erosion, and the subgrid-scale fluvial erosion must be characterized. Conventional treatment of hillslope runoff divides the flow and sediment transport into unconcentrated (interrill, overland, sheetwash) and channelized (rill) modes (see review by *Abrahams et al.* [1994]). On vegetated slopes little erosion occurs until downslope flow accumulation reaches a threshold stress capable of disturbing the vegetation mat, so that runoff erosion is essentially

restricted to ephemeral or perennial rills and gullies [e.g., *Dietrich et al.*, 1993]. On badlands and shale slopes runoff often occurs as interflow through shrinkage cracks and small pipes [*Hodges and Bryan*, 1982; *Bryan et al.*, 1984; *Gerits et al.*, 1987; *Imeson and Verstraten*, 1988], reemerging into the exposed rill network. On exposed sandy slopes, such as agricultural fields, erosion by unconcentrated flow may be appreciable, although the observations from experimental plots exaggerate overland flow erosion because of unnatural initial conditions (a smoothed rather than the rilled surface that would often evolve if left to natural processes). In addition, a considerable proportion of the water erosion may be due to rain splash, which is a diffusive process [*Ahnert*, 1976; *Kirkby*, 1976b, 1987; *Dunne and Aubrey*, 1986] and may be included under the mass wasting mathematical modeling. Even where overland flow occurs, it is generally not uniform but concentrated into shallow channels lacking well-defined banks [*Abrahams et al.*, 1994]. This model assumes that runoff erosion occurs only in channelized flow.

On natural headwater slopes there might be several ephemeral rills within the area represented by one simulation grid cell, but it is assumed that all runoff becomes concentrated into a single permanent or ephemeral channel running the length of the cell with a gradient equal to the overall slope gradient and that all fluvial erosion within the cell occurs in this channel. Erosion by runoff will be somewhat exaggerated in the present model because of the scale efficiency associated with a single channel rather than multiple small channels. Nonetheless, channel erosion becomes negligible compared with mass wasting on matrix cells located near divides.

As with most quantitative models of landform evolution, local vertical rate of land surface elevation change $\partial y/\partial t$ is related to local tectonic uplift rate U and the spatial divergence of the vector of eroded material flux $\mathbf{q}$ (volume per unit width of slope or channel):

$$\partial y/\partial t - U = \partial z/\partial t = -\nabla \cdot \mathbf{q}, \tag{4}$$

where $\partial z/\partial t$ is erosion rate relative to a bedrock-fixed reference frame. The volumetric transport can result from a variety of processes, including solute transport, mass movement, and fluvial transport. In general, there should also be a correction for changes of rock volume on conversion to regolith [*Carson and Kirkby*, 1972, p. 107], which is ignored here. Only diffusive rain splash and mass wasting and concentrative fluvial transport are considered in the present model. Process rate laws for these are considered below in terms of potential splash and mass wasting $\partial z/\partial t|_m$ and fluvial $\partial z/\partial t|_c$ erosion rates. Because each simulation cell may contain variable proportions of channel and slope components, the actual local erosion rate is a weighted sum of the potential rates.

Weathering, Rain Splash, and Mass Movement

Weathering is not explicitly modeled, but is assumed to keep pace with erosion by rain splash, mass wasting, or fluvial processes such that everywhere except in some channels there is a weathered, cohesive regolith. Creep or slope failure is assumed to occur at a sufficiently shallow depth with regard to the thickness of the regolith that its thickness is not a limiting factor. Measurements of creep rates below slopes with well-developed regolith generally show most movement occurring close to the surface (see review by *Carson and Kirkby* [1972]). Similar assumptions have been made in a number of quantitative slope evolution models [*Ahnert*, 1976, 1987a; *Armstrong*, 1976; *Kirkby*, 1986, 1987; *Willgoose et al.*, 1991a, b, c].

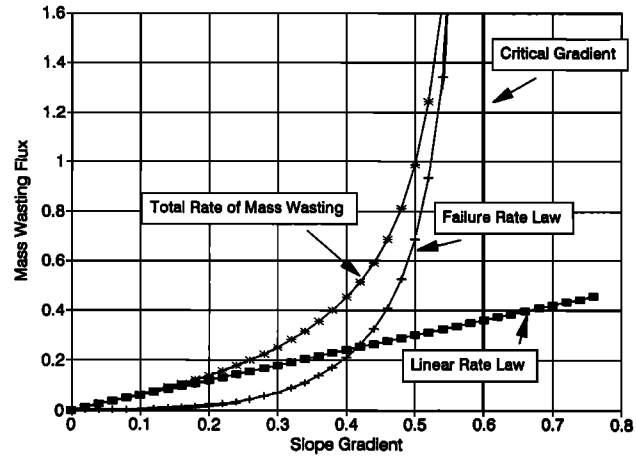

Figure 1. Example of mass wasting flux predicted by (6) when both terms contribute.

Potential erosion or deposition due to rain splash and regolith mass movement is given by the spatial divergence of the vector rate of movement $\mathbf{q}_m$:

$$\left.\frac{\partial z}{\partial t}\right|_m = -\nabla \cdot \mathbf{q}_m. \tag{5}$$

The rate of movement is expressed by two additive terms, one for creep and/or rain splash diffusion and one for near-failure conditions (e.g., Figure 1):

$$\mathbf{q}_m = \left[K_s \mathcal{G}(S) + K_f \frac{1}{(1 - K_x|S|^a)}\right]\mathbf{s}, \tag{6}$$

where $\mathcal{G}(S)$ is an increasing function of slope gradient, $\mathbf{s}$ is the unit vector in the direction of $\mathbf{S}$, and $|S|$ is the absolute value of local slope gradient. The constants K_s, K_x, K_f, and the exponent a are constants assumed to be spatially and temporally invariant. Simple analysis of rain splash or creep driven by gravity suggests that the function $\mathcal{G}(S)$ would be the sine of the slope angle θ:

$$\mathcal{G}(S) = \sin \theta. \tag{7}$$

However, the present model assumes a linear dependency:

$$\mathcal{G}(S) = \tan \theta = S. \tag{8}$$

In addition, for most of the simulations, K_f is assumed to be zero, so that the right side of (5) simplifies to the Laplacian of elevation, $K_s \nabla^2 z$. The model of *Willgoose et al.* [1991a, b, c] also assumes diffusive erosion proportional to the Laplacian of elevation.

The second term in the brackets of (6) models near-failure conditions on slopes such that mass movement rates increase without limit as gradient approaches a threshold value equal to $(1/K_x)^{1/a}$. *Kirkby* [1984, 1985b, 1987] provides a more comprehensive formulation for landslide and talus mass movement that accounts for flow kinematics.

The spatial divergence in (5) is evaluated in eight directions. Relative weighting of one third for diagonal terms and two thirds for cross terms is used, equivalent to the nine-point finite difference weights for the Laplacian [*Gerald and Wheatley*, 1989].

Fluvial Processes

The model incorporates both detachment-limited erosion on slopes and steep headwater channels as well as sediment transport in alluvial channels. Potential channel deposition or erosion $\partial z/\partial t|_c$ depends upon whether the channel is alluvial or nonalluvial and is proportional to the spatial divergence of sediment transport flux, $\mathbf{q}_s$:

$$\left.\frac{\partial z}{\partial t}\right|_c = -\nabla \cdot \mathbf{q}_s = -\frac{\partial q_s}{\partial x}, \tag{9}$$

where q_s is the volumetric sediment transport rate per unit channel width, and the downstream direction is x (fluvial flows are assumed to be well-channelized and nearly uniform). The sediment discharge is broken down into wash load q_{sw}, which is assumed to never be redeposited except in depressions, and bed sediment (bed load and suspended load) q_{sb}, which is carried in capacity amounts if an alluvial bed is present. If the channel is alluvial, then q_{sb} is predicted from sediment transport relationships. For nonalluvial channels the transport divergence $\partial q_s/\partial x$ is given by an intrinsic detachment capacity (volume per unit area per unit time) C_d.

Nonalluvial channels. In the present context, a nonalluvial channel is defined as one in which the bed load sediment flux is less than a capacity load. Such channels may be flowing on bedrock or on regolith. The detachment capacity in nonalluvial channels is assumed to be proportional to the shear stress τ exerted on the bed and banks by a dominant discharge:

$$-\left.\frac{\partial z}{\partial t}\right|_c = \frac{\partial q_s}{\partial x} = C_d = K_t(\tau - \tau_c), \tag{10}$$

where τ_c is a critical shear stress, which should be larger than the critical shear stress for noncohesive sediment entrainment. *Foster and Meyer* [1972], *Meyer* [1986], *Lane et al.* [1988], and *Foster* [1990] suggest that the actual detachment rate C decreases from the intrinsic detachment capacity C_d (for zero sediment load) to zero as the actual bed sediment transport rate approaches the flow transport capacity. This approach is appropriate for slopes and channels floored with cohesionless sediment, but the implied interaction between deposition and entrainment is not relevant to water erosion of cohesive regolith or bedrock.

Shear stress can be related to channel gradient and drainage area through the use of equations of steady, uniform flow:

$$\tau = \gamma RS \tag{11}$$

$$V = K_n R^{2/3} S^{1/2}/N \tag{12}$$

$$Q_w = K_p RWV \tag{13}$$

where γ is the unit weight of water, R is the hydraulic radius, N is Manning's resistance coefficient, K_n is unity in m s units and 1.5 in foot s units, and K_p is a form factor close to unity. The model also assume simple power law equations of hydraulic geometry for dominant discharge Q_w (assumed to be equal for both bed erosion and sediment transport) and channel width W:

$$Q_w = K_a A^e, \tag{14}$$

$$W = K_w Q_w^b = K_w K_a^b A^{be}. \tag{15}$$

The use of an equation such as (14) for runoff on slopes as well as in channels implies that little regolith or depression storage of precipitation occurs during erosion events, since runoff production is assumed to be areally uniform. On badland slopes this is probably a reasonable approximation. For landscapes with appreciable infiltration capacity, particularly where vegetated, the assumption is made that most runoff erosion on slopes occurs during infrequent, very intense rainfall events due to saturation overland flow or shallow interflow through large macropores. *Kirkby* [1987] outlines a slope development model that accounts for infiltration and partial contributing areas.

Combining (10) with (11)–(15) gives

$$\partial z/\partial t|_c = -K_t(K_z A^g S^h - \tau_c), \tag{16a}$$

where

$$g = 0.6e(1 - b), \tag{16b}$$

$$h = 0.7, \tag{16c}$$

$$K_z = \gamma\left\{\frac{NK_a^{(1-b)}}{K_p K_w K_n}\right\}^{3/5}. \tag{16d}$$

The constant K_t in (16a) includes both effects of substrate erodibility as well as magnitude of the dominant discharge. Channels may be eroding both regolith material which is delivered into the channel by mass wasting as well as uneroded bedrock. Regolith material is assumed to be more erodible than bedrock by a factor F, where $F \geq 1$. The fluvial erosion rate for bedrock is given by (16a), so that the equivalent rate for regolith is $F\ \partial z/\partial t|_c$. The critical shear stress τ_c might also depend upon substrate type (bedrock or regolith), although in the present modeling it is assigned a fixed value.

In landscapes with a shallow weathering regolith, such as in badlands and steep mountain slopes, bedrock is commonly exposed in headwater rills and channels, and a large ratio of bedrock to regolith erodibility ($F \gg 1$) would be appropriate. However, in landscapes in deeply saprolitized bedrock, till, or uncemented alluvium, the parent material and the surface soil involved in mass wasting may have nearly equivalent erodibility ($F \sim 1$).

In calculating net erosion in matrix cells containing nonalluvial channels it is necessary to take into account that erosion is occurring in a channel of width W and that the channel may be eroding both regolith and bedrock during a given time step. The eroded regolith comprises both that delivered by mass wasting into the cell from the adjacent cells and that which is locally derived. During each time step the channel is assumed to erode first regolith delivered to the channel by slope erosion and then, if it is capable of eroding all regolith, bedrock. The fraction of time during each time step that the channel is eroding regolith is η ($0 \leq \eta \leq 1$). There are three cases, the simplest of which occurs when sufficiently large amount of regolith is delivered to the cell

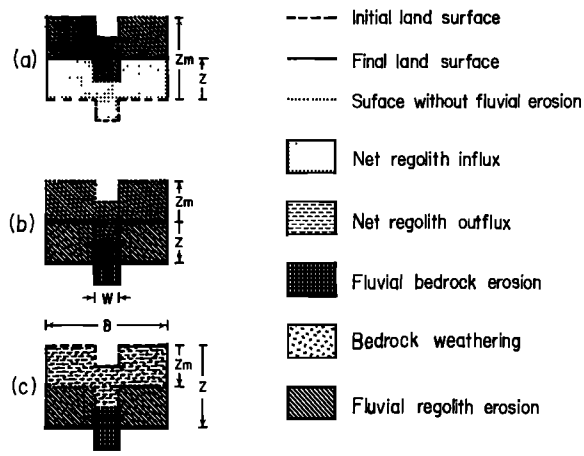

Figure 2. Conceptual cross sections through simulation cells perpendicular to stream channel of width W partially occupying the cell of width δ, showing changes during one simulation time step. The three cases illustrate different situations with regard to the relative roles of mass wasting and fluvial erosion and also differences in the amount of direct bedrock scour by the channel. (a) Mass-wasting influx exceeds fluvial erosion potential, and the landscape increases in elevation (corresponding to (17). (b) Net mass-wasting influx, but fluvial erosion is capable of eroding mass-wasted debris, locally weathered regolith, and the bedrock floor of the channel (21). (c) As in Figure 2b, but with a net mass-wasting efflux from the cell (24). Note that intracell topography is not explicitly modeled. Zm is the potential slope erosion $\partial z/\partial t|_m$, and Z is the net actual erosion $\partial z/\partial t$. Dotted lines show surface that would result if fluvial erosion did not occur.

that the channel never erodes bedrock ($\eta = 1$). The volume of regolith delivered to the cell per unit time is $\partial z/\partial t|_m\ \delta^2$, and the volume of channel erosion is $(FLW\ \partial z/\partial t|_c)$. The length L of the channel in the cell is assumed to be δ. The net elevation change $\partial z/\partial t$ is the sum of the volume of regolith mass movement and of volumetric channel erosion divided by the area of the cell (Figure 2a):

$$\frac{\partial z}{\partial t} = \left.\frac{\partial z}{\partial t}\right|_m + F\xi \left.\frac{\partial z}{\partial t}\right|_c, \tag{17a}$$

where

$$\xi = W/\delta. \tag{17b}$$

The criterion for (17a) to pertain is that $\partial z/\partial t \geq 0$.

If the channel is capable of eroding all regolith delivered to it, then the value of η must be determined. Weathering is assumed to be capable of keeping pace with the net rate $\partial z/\partial t$ of lowering of the land (and bedrock surface), so that the net volumetric rate of regolith production and delivery by mass wasting to the channel for erosion ε is (Figure 2b):

$$\varepsilon = \left.\frac{\partial z}{\partial t}\right|_m \delta^2 - \frac{\partial z}{\partial t}\,\delta(\delta - W), \tag{18}$$

where the first term is the regolith volume imported from adjacent cells, and the second term accounts for the within-cell contribution from weathering adjacent to the channel. The fraction of time the channel spends eroding regolith is

$$\eta = -\frac{\varepsilon}{F\xi\delta^2 \left.\dfrac{\partial z}{\partial t}\right|_c}, \tag{19}$$

since the denominator is the (negative of the) maximum volume of regolith that can be eroded per unit time by the channel. The net erosion (into bedrock) is also given by

$$\frac{\partial z}{\partial t} = (1 - \eta) \left.\frac{\partial z}{\partial c}\right|_c. \tag{20}$$

Substituting (18) and (19) into (20) to eliminate η:

$$\frac{\partial z}{\partial t} = \beta\left\{\left.\frac{\partial z}{\partial t}\right|_m + F\xi \left.\frac{\partial z}{\partial t}\right|_c\right\}, \tag{21a}$$

where

$$\beta = 1/(F\xi + 1 - \xi). \tag{21b}$$

This relationship pertains so long as $\partial z/\partial t|_m \geq 0$ and $\partial z/\partial t < 0$.

The final case, where $\partial z/\partial t|_m < 0$, is similar, except it is assumed that removal of regolith by channel erosion pertains only to the volume surrounding the stream and below the level of removal by slope erosion, that is (Figure 2c),

$$\varepsilon = \left\{\left.\frac{\partial z}{\partial t}\right|_m - \frac{\partial z}{\partial t}\right\}\delta(\delta - W), \tag{22}$$

and the net erosion into bedrock is given by

$$\left\{\left.\frac{\partial z}{\partial t}\right|_m - \frac{\partial z}{\partial t}\right\} = (1 - \eta) \left.\frac{\partial z}{\partial t}\right|_c. \tag{23}$$

The analysis proceeds as with the previous case, giving

$$\frac{\partial z}{\partial t} = \left.\frac{\partial z}{\partial t}\right|_m + \beta F\xi \left.\frac{\partial z}{\partial t}\right|_c. \tag{24}$$

This series of relationships (17), (21), and (24) provides a continuous functional dependence of erosion rate upon $\partial z/\partial t|_m$ and $\partial z/\partial t|_c$ but with changes of slope at $\partial z/\partial t = 0$ and $\partial z/\partial t|_m = 0$ in the general case (Figure 3).

Alluvial channels. For alluvial channels the potential rate of fluvial erosion equals the spatial divergence of the volumetric unit bed sediment transport rate $\mathbf{q}_{sb}$:

$$\left.\frac{\partial z}{\partial t}\right|_c = -\nabla \cdot \mathbf{q}_{sb}. \tag{25}$$

Many bed load and total load sediment transport equations for sediment discharge can be expressed as a functional relationship between the two parameters dimensionless parameters ϕ and $1/\Psi$:

$$\phi = \mathcal{F}\left(\frac{1}{\Psi}\right), \tag{26a}$$

where

$$\phi = \frac{q_{sb}}{\omega d(1 - \mu)}, \qquad \frac{1}{\Psi} = \frac{\tau}{(\gamma_s - \gamma)d}. \tag{26b}$$

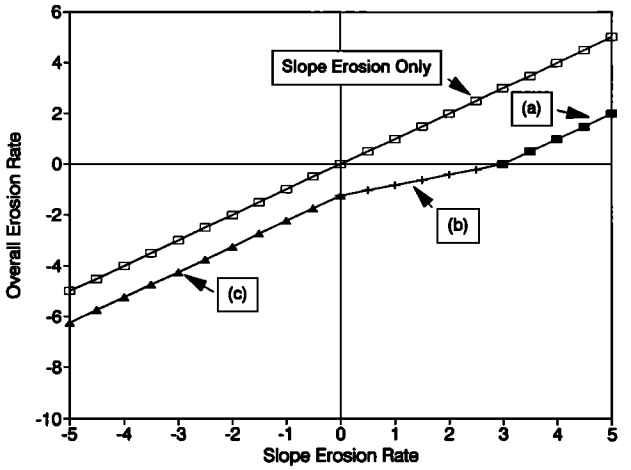

Figure 3. Graph of overall erosion rate $\partial z/\partial t$ as a function of potential slope erosion rate $\partial z/\partial t|_m$ and potential channel erosion rate $\partial z/\partial t|_c$, illustrating the three cases a, b, and c in Figure 2. For this illustration $\partial z/\partial t|_c = -2.0$, $F = 15$, and $\xi = 0.1$.

In these equations, q_{sb} is bed sediment transport rate in bulk volume of sediment per unit time per unit channel width, ω is the fall velocity of the sediment grains, d is the sediment grain size, μ is alluvium porosity, and γ_s is the unit weight of sediment grains. Bed load or total load formulas are commonly expressed as a power function relationship:

$$\phi = K_e\left\{\frac{1}{\Psi} - \frac{1}{\Psi_c}\right\}^p, \tag{27}$$

where $1/\Psi_c$ is the threshold for transport. For sand bed channels with high effective discharges, the exponent p in total load formulas is generally about 3, and $1/\Psi_c$ is a negligible correction. As was discussed by *Howard* [1980] and *Willgoose et al.* [1991a], this equation can be recast into a relationship between total bed sediment discharge Q_{sb} ($q_{sb}W$), drainage area, and gradient using (26), (27), and (11)–(15):

$$Q_{sb} = K_q A^{eb}[K_v A^{0.6e(1-b)} S^{0.7} - 1/\Psi_c]^p, \tag{28a}$$

where

$$K_q = \frac{K_e\omega(1-\mu)K_w K_a^b}{(\gamma_s - \gamma)^p d^{p-1}} \tag{28b}$$

$$K_v = \gamma\left\{\frac{NK_a^{1-b}}{K_w K_n K_p}\right\}^{0.6}. \tag{28c}$$

In evaluating the sediment divergence, it is assumed that all sediment transporting flows occur in channels with local width W given by (15). The net erosion is therefore given by the following relationship between the total sediment influx into Q_{sbi} and outflow from Q_{sbo} a given cell:

$$\left.\frac{\partial z}{\partial t}\right|_c = \frac{(Q_{sbi} - Q_{sbo})}{LW}, \tag{29}$$

where L is the length of the channel through the cell. Several adjacent cells may contribute to the sediment influx to a cell, but the outflux occurs to the adjacent cell with the steepest downslope gradient. In the case of a depression there is no outflux. Influxes may originate from alluvial streams debauching into the cell from adjoining cells or from nonalluvial streams and rills. In the latter case the incoming Q_{sbi} equals the total volume of upstream nonalluvial channel erosion less the proportion of load carried as wash load, corresponding to the assumption that downstream routing of sediment through nonalluvial channels is very rapid compared to the iteration time step.

Although alluvial transport is assumed to occur in well-defined channels whose width is less than the simulation cell width, over long periods of time the channel is assumed to erode or deposit over the entire area of the cell, so that the divisor LW in (29) becomes the area of the cell, δ^2. However, the channel width used in (28) to calculate transport capacity is the local channel width W (equation (15)).

The implementation of the differential equations governing erosion (4), (5), (16), (17), (21), (24), and (25) is generally straightforward finite difference approximation (e.g., (29)). A primary concern is selection of a temporal increment that assures numerical stability. Each of the processes outlined above has a characteristic maximum time step, and the overall model must utilize the minimum of these. However, the maximum time step for sediment transport divergence erosion (29) is less by a factor of 10^3 to 10^4 than that for slope or bedrock channel erosion. This occurs primarily for channels with large drainage area and low gradient. Because the exponent of gradient in (28) is ≈ 2, small changes in gradient create large variations in transport rate so that time steps must be very small to assure that numerical errors are not amplified. *Willgoose* [1989] utilizes a predictor-corrector numerical algorithm to maximize allowable time steps, but computational burdens are still very high.

An alternative approach is used here for alluvial channels with large drainage areas, which permits simulation of alluvial channel evolution using workstations rather than supercomputers. The timescale for alluvial channel regrading due to changes in supply of sediment or water from upstream or due to local uplift base level changes is assumed to be short compared to that for overall evolution of basin relief. The short timescale of alluvial channel regrading is manifest in many drainage basins by the often multifold deposition and dissection of terraces in response to changes in hydraulic regime over time periods during which overall basin relief has changed very little. The approach is to utilize the longer time step Δt which is appropriate for slope and bedrock channel erosion, thus ignoring the type of short-term fluctuations responsible for terraces.

At the head of each section of alluvial channel a discharge of sediment Q_{sj} is delivered by upstream channel erosion, making a volumetric contribution of $Q_{sj}\Delta t$ during each time step; the subscript j is used because each channel or slope draining into the alluvial channel contributes individually to the overall sediment discharge Q_s. This volumetric contribution is routed downstream, in general, being deposited within n segments (elements) of the alluvial channel system. If Z_i is the mean elevation of a given alluvial segment, then the overall volume V of the alluvial channel between the nonalluvial upstream node at elevation Z_0 and the downstream unmodified node with elevation E_{n+1} is

$$V = 0.5\delta^2[(Z_0 + Z_1) + (Z_1 + Z_2) + \cdots + (Z_n + Z_{n+1})]. \quad (30)$$

Since $Z_1 = Z_0 - S_0 l_0$ and $Z_2 = Z_1 - S_1 l_1$, etc., where S_i is the gradient and l_i is the length of each channel segment (δ or $2^{1/2}\delta$ depending upon whether the channel is parallel to a matrix edge or diagonal),

$$V = \delta^2\left[\left(n + \frac{1}{2}\right)Z_0 - nS_0l_0 - \sum_{i=1}^{n-1}(n-i)S_il_i + \frac{1}{2}Z_{n+1}\right]. \quad (31)$$

A parallel expression can be written for the volume $\mathcal{V}$ that occurs at the end of the time step, with $\mathcal{T}_i$ representing the final elevations and $\mathcal{S}_i$ the final gradients. The net deposited volume of sediment for an individual nonalluvial upstream contribution during the time step equals the difference between the two volumes:

$$Q_{sj}\Delta t = \mathcal{V} - V. \quad (32)$$

The final gradients $\mathcal{S}_i$ of the alluvial channel nodes ($1 \cdots n$) are the steady state gradients given by solving (28) for gradient using the total nonalluvial sediment contribution Q_s upstream from each node. The solution marches downstream, initially assuming $n = 1$ and that the elevations Z_0 and Z_{n+1} are fixed, solving (32) for the gradients $\mathcal{S}_0$ and $\mathcal{S}_n$ by substituting (31) and the parallel expression for $\mathcal{V}$:

$$\mathcal{S}_0 = S_0 - \left[\sum_{i=1}^{n-1}(n-i)(S_i - \mathcal{S}_i)l_i + (Q_{sj}\Delta t)/\delta^2\right] \Big/ [nl_0], \quad (33)$$

$$\mathcal{S}_n = \left[(Z_0 - Z_{n+1}) - \mathcal{S}_0 l_0 - \sum_{i=1}^{n-1}\mathcal{S}_i l_i\right] \Big/ l_n. \quad (34)$$

The calculation proceeds iteratively, increasing n until one of the following occurs: (1) the gradient of the final segment $\mathcal{S}_n$ is less than or equal to the steady state alluvial gradient for the local drainage area and total sediment discharge, or (2) location n is a fixed boundary point with elevation Z_f. In the former case all of the bed sediment supplied from upstream is deposited, and the new elevations $\mathcal{T}_i$ of the alluvial channel points are calculated from

$$\mathcal{T}_i = Z_0 - \mathcal{S}_0 l_0 - \sum_{k=1}^{i-1}\mathcal{S}_k l_k. \quad (35)$$

In the latter case, the channel is graded upstream from the fixed boundary point, with the assumption that undeposited sediment load is carried from the system, so that

$$\mathcal{T}_i = Z_f + \sum_{k=n-1}^{i+1}\mathcal{S}_k l_k, \quad (36)$$

where the index k is decremented.

Special treatment is required for deltaic deposition into a water-filled depression or sea. Submerged alluvial bed sediment deposits are assumed to be foreset beds with an angle of repose gradient of $\mathcal{S}_r$. The routing scheme takes into consideration that a channel segment with a subareal upstream node and a submerged downstream node will have a portion of the segment having gradient $\mathcal{S}_i$ and part with gradient $\mathcal{S}_r$.

Another special circumstance occurs for the first case when one or more of the downstream locations is nonalluvial. If one of these locations is nonalluvial and the predicted new elevation $\mathcal{T}_i$ is less than the existing elevation Z_i, then the alluvial channel is backgraded from the existing elevation using a formula similar to (36), and bed sediment that is not deposited is routed further downstream through the bedrock section.

Since many nonalluvial slopes and channels may each contribute sediment $Q_{sj}\Delta t$ during each time step, the calculation is repeated for each of these sources, with each previously calculated new elevation $\mathcal{T}_i$, now becoming the initial elevation Z_i for the new source. Thus alluvial channels may undergo several subiterations of deposition during each time step.

Finally, the upstream location at Z_0 is converted to an alluvial channel if the calculated new gradient $\mathcal{S}_0$ is less than the steady state alluvial gradient calculated using (28).

This routing procedure is used for all alluvial channel nodes except for those which do not lie along the path of sediment routing from an upstream nonalluvial channel during a given iteration; such nodes are regraded using the finite difference approximation (29). In addition, the finite difference solution is used for those few alluvial nodes that both (1) lie immediately downstream from a bedrock channel and (2) have zero sediment transport rate from (28).

The accuracy of this routing technique was validated by simulations of stream profiles using both the routing scheme and traditional finite difference techniques; simulated profiles were nearly identical, even in the case of initially nonalluvial channels being replaced by retrograding alluvial channels after the base level is fixed (similar to the two-dimensional simulations shown in Figure 18).

Transitions. All cells in the simulation matrix have a contribution to erosion or deposition from either an alluvial or a nonalluvial channel, but the two types of channels are mutually exclusive. Thus the model must provide criteria for temporal and spatial transitions.

If the channel in a cell is currently nonalluvial, the sediment arriving from upstream and that locally eroded by the channel is considered to be transported without deposition and to be routed instantaneously (relative to the simulation timescale) through the nonalluvial network. During each iteration the total potential bedload transport capacity of the channel in each cell is calculated (using (28)), and if the actual transport rate exceeds the potential rate, then the cell is converted to an alluvial channel. When such a transition occurs the base of the alluvial deposit is set equal to the local elevation.

So long as erosion due to sediment divergence in an alluvial channel during an iteration is less than the thickness of the alluvium, the channel remains alluvial. However, alluvial channels in nature and in the model may also occur under conditions of slow downcutting (such that the base of the alluvial deposit is constantly reset during each iteration to the local elevation). The maximum amount of erosion that an alluvial channel on shallow alluvium over bedrock can accomplish is considered to equal the rate for nonalluvial

channels into bedrock ($\partial z/\partial t|_c$, given by (16)). If the erosion due to sediment divergence (using (29) or the routing procedure of (30)–(36)) exceeds this value within a channel on shallow alluvium, then the channel is converted to a nonalluvial channel.

Simulation Procedures

The simulations reported here are conducted on a 100 × 100 square matrix. Distances and areas are scaled using an assumed unity cell size and a contributing area of unity to each cell. In internal cells, drainage and mass wasting may occur toward any of the eight neighboring cells. Sediment and discharge leave each cell only toward that cell with the steepest downslope gradient, taking into account the difference in distance toward diagonal cells. However, calculation of mass-wasting flux divergence is based upon relative elevations of the matrix point and of the eight surrounding points. Drainage areas are determined by accumulating flow downslope and downchannel, with each matrix element contributing a unit drainage area.

Three types of boundary cells exist. The lower matrix edge is assumed to be a level surface of specified elevation. For simulations of steady state drainage basin development this lower edge is lowered at a constant rate $\partial z/\partial t|_b$. This matrix edge is the controlling base level and can generally be considered to be a master drainage line of negligibly small gradient. Lateral matrix edges are periodic; water, regolith, or sediment moving across, say, the left boundary is reintroduced across the right boundary, and calculation of gradients and divergences consider the two edges to be adjacent. The upper row of matrix cells is assumed to be impenetrable by water, regolith, or sediment. In most cases this boundary accordingly becomes a drainage divide, although it can also lie along a channel (e.g., part of the upper boundary in Figure 12b).

A variety of initial conditions are utilized in the simulations. Most simulations start from a nearly planar surface that has a superimposed quasi-fractal random elevation variation generated in a manner similar to that described by *Kirkby* [1986a, b]. The influence of initial conditions on basin morphology is discussed below.

Because of the random elevation component, depressions may exist. The influence of depressions upon mass wasting is automatically accounted for in the calculation of gradient divergence (5). Two endpoint behaviors of water flow and sediment transport are considered. In the first, "dry," case, water reaching the bottom of an enclosed depression disappears (corresponding to flow volumes being unable to fill the depression during a runoff event) and sediment in transport is deposited at the lowest point of the depression. In the "wet" case, flow fills the depression to overflowing, and lakes occur on the surface. Fluvial sediment entering a lake is immediately deposited, but water flow is routed downstream without loss; no fluvial transport or scour can occur within lakes. All simulations reported here assume the wet case. In steady state simulations, initial enclosed depressions disappear rapidly.

Generally, the bedrock and regolith erosional susceptibility and the water runoff yield are assumed to be spatially uniform and temporally constant. Individual flow events are not modeled, and it is assumed that the erosional and sediment transport potential of the calculated discharges, parameterized as a function of drainage area only, can be characterized by a temporally constant "dominant" discharge representing the integrated effect of the time-varying flows in nature.

The simulation proceeds by iterations with a specified time increment, and rates of mass wasting, sediment transport, and fluvial bedrock erosion scaled by the relationships presented above. Gradients and drainage areas, as well as depth and flow outlets of enclosed depressions, are recalculated after each iteration.

The selection of spatial and temporal scales is an important concern in simulation modeling. The time step is selected so that the solution is numerically stable and that further decrease in the time step does not alter the resulting landforms. The spatial scale of the simulated landscape is determined by the relative values of the mass wasting (K_s and K_t in (6)) and fluvial (K_t and K_z in (16)) constants of proportionality. Depending upon the selected constants, the simulated landscape can have numerous or few channels. The simulations shown here utilize fluvial and mass-wasting constants that give a high drainage density while adequately representing divide convexity.

Results

Simulations have been conducted with a range of model parameter values and a variety of initial and boundary conditions. These simulations have implications with regard to several important issues in drainage basin morphology and evolution, including inheritance from initial conditions, the roles of random and chaotic processes, definition of drainage density, model validation, and optimality principles applied to drainage basin evolution.

Steady State Simulations With No Alluvial Channels

A simple and informative type of simulation involves a steady rate of lowering of the lower boundary, representing either a constant rate of base level drop or constant rate of uplift with a fixed location of base level. Under these conditions a steady state topography eventually develops from any initial conditions in which all parts of the landscape erode vertically at a constant rate. Furthermore, gradients and slope orientations become constant, and the fluvial drainage network becomes fixed. Actually, because some cells have essentially equal gradients toward two or more adjacent cells, a few oscillations of the drainage directions occur on slopes, but these are imperceptible in the topographic maps (e.g., Figure 4) or summary statistics of basin morphology. Illustrative examples of steady state basin morphology for various combinations of model parameters are discussed below. Values of simulation parameters are presented in Table 1. All of these steady state simulations assume that the entire channel network is nonalluvial.

The simplest model. Although the model provides a general framework for slope and channel evolution in regolith-mantled environments, one purpose of this modeling is to ascertain the mathematically simplest models that are physically reasonable and can produce realistic topography. One such case occurs when all channels are nonalluvial, when there is no critical shear stress and no near-failure contribution to slope erosion, and when regolith and bedrock are equally erodible ($F = 1$). In this case, (17), (21), and (24) simplify to

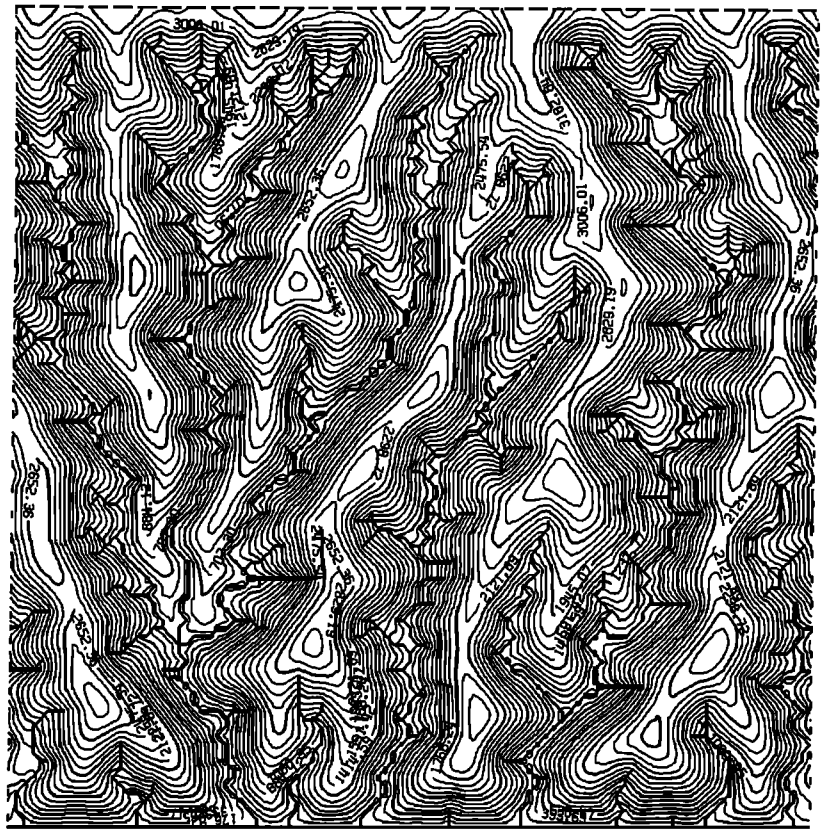

Figure 4. Simulated steady state landscape produced by simulation model for $F = 1$ and no critical shear stress. Erosion is governed by (38). Note that simulation is not scaled to any particular natural landscape; both horizontal and vertical scales in this and the other simulations should be considered to be arbitrary.

$$\frac{\partial z}{\partial t} = \left.\frac{\partial z}{\partial t}\right|_m + \xi \left.\frac{\partial z}{\partial t}\right|_c, \tag{37}$$

and substituting from (5), (6), (8), (15), (16), and (17b),

$$\partial z/\partial t = -\nabla^2 z - \delta^{-1} K_w K_a^b K_t K_z A^{e(0.6+0.4b)} S^{0.7}. \tag{38}$$

Thus the erosion rate is a linear combination of a diffusive mass-wasting term (the Laplacian) which tends to smooth the topography and channel erosion term which becomes more important (for a given gradient) as drainage area increases. All cells have some contribution of fluvial erosion and mass wasting.

Table 1. Parameters for Simulation Runs

	Parameter and Defining Equation					
Figures	$K_t K_z$ (16)	K_s (6)	F (17)	$K_t \tau_c$ (16)	m (16)	n (16)
4	1.0	0.004	1.0	0.0	0.3	0.7
6, 10, 11, 13a–13c and 16	1.0	1.0	500.0	0.0	0.3	0.7
7	1.0	1.0	500.0	5.0	0.3	0.7
8*	1.0	0.1	500.0	0.0	0.3	0.7
12a	1.7	1.0	500.0	0.0	0.18	1.18
12b	1.0	7.0	500.0	0.0	1.0	1.0
17†	1.0	0.1	50.0	0.0	0.3	0.7
18‡	1.0	3.0	500.0	0.0	0.3	0.7

All simulations assume $\delta = 1$, $K_w K_a^b = 0.005$ (equation (15)), $be = 0.5$ (equation (15)), and $\mathcal{G}(S) = S$ (equation (8)). Steady state simulations assume $\partial z/\partial t = -1.0$ at lower matrix edge.

*Threshold slope parameters in (6) are $K_f = 0.5$, $K_x = 4.63$, and $\alpha = 3.0$, giving a threshold gradient of 0.6.

†Sediment transport parameters in (28) are $K_q = 500.0$, $K_v = 1$, $e = 0.6$, $b = 0.5$, $p = 3.0$, and $1/\Psi_c = 1.3$.

‡Sediment transport parameters in (28) are $K_q = 100.0$, K_v 1, $e = 1.0$, $b = 0.5$, $p = 3.0$, and $1/\Psi_c = 0.0$.

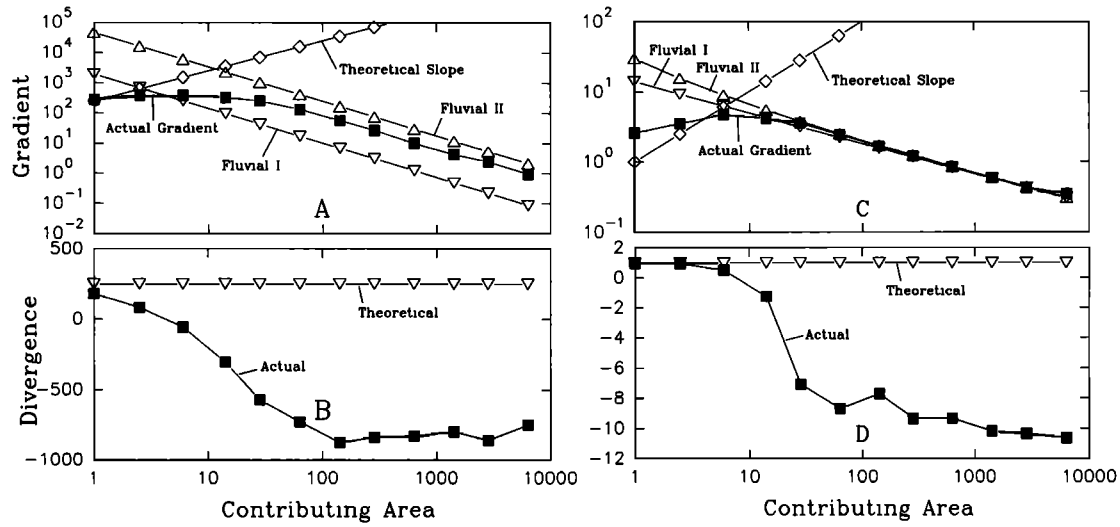

Figure 5. Plots of actual and theoretical values of gradient (Figures 5a and 5c) and divergence (Figures 5b and 5d) as a function of contributing area for the simulations in Figure 4 (Figures 5a and 5b) and Figure 6 (Figures 5c and 5d).

Figure 4 shows a steady state drainage basin resulting from these assumptions. Steady state solutions to (38) result in landscapes partitioned into a majority of cells in which the diffusive term dominates (the slopes and divides) and a dendritic valley network dominated by fluvial erosion. The simulation model does not directly specify the location of stream channels; rather, channel locations result from the interaction of the two terms in (38) with the initial random topography.

The relative influence of the two terms in (38) can be illustrated by plotting average land surface gradient and slope divergence versus contributing area (Figures 5a and 5b). Each graphed point is the average gradient or divergence for matrix cells having drainage areas within the (logarithmic) range surrounding each area interval. The form of the relationship showing a peak gradient value at a certain contributing area has been noted in digital elevation data from natural drainage basins [*Willgoose et al.*, 1992; *Tarboton et al.*, 1992] and in the simulation model of *Willgoose et al.* [1991d]. Four limiting theoretical curves are shown in Figures 5a and 5b. The "theoretical slope" curve shows the gradients that would be necessary on a one-dimensional slope profile for diffusional mass wasting or rain splash to produce the steady state erosion rate (i.e., if only the first term in (38) were important). Because of two-dimensional divergence and erosion attributable to term 2 in (38), this theoretical curve predicts gradients larger than are observed, except at divides (contributing area equal to unity). Figure 5b shows the actual slope gradient divergences ($\nabla^2 z$) and the theoretical value (which is independent of drainage area) that would be required for erosion entirely by diffusion. Except close to divides, the actual slope divergence is much less than the theoretical value because of the erosional contribution of the second term in (38).

Two additional theoretical curves are shown in Figure 5a. These are gradients that would be expected downstream where fluvial erosion dominates. The lower of the two curves shows gradients that would occur if only the second term in (38) were important in fluvial erosion, that is, if channels did not have to erode regolith. Clearly, some contribution of the first term occurs in the simulated landscape even in the larger channels. The upper curve assumes that both terms in (38) are important and that the volume of regolith delivered to each unit length of channel per unit time equals the total volumetric erosion rate divided by the total length of the valley network (as defined by the criterion discussed below). The actual gradient curve falls somewhat below this second curve because some fluvial erosion of regolith occurs on slopes upstream from the drainage sources.

Strongly erodible regolith. The next most simple combination of model parameters occurs when the regolith is much more erodible than bedrock, that is, when the parameter F is large. Figure 6 shows a steady state solution in which F = 500. Because of the multiple solution cases implied in (17), (21), and (24), a single governing differential equation cannot be written. However, a strong trade-off occurs between dominance by diffusive slope erosion near divides ($\partial z/\partial t|_m$ in (5)) and dominance by channel erosion downstream ($\partial z/\partial t|_c$ in (16)). This is illustrated in the gradient and divergence versus contributing area graph (Figures 5c and 5d). The portions of the graph near the divides (small contributing area) are similar to the pattern seen in Figures 5a and 5b. However, owing to the negligible influence of regolith influx in determining erosion rates in larger channels, the theoretical curve for no contribution from regolith influx is a very close approximation to the simulated gradients on the right side of Figure 5c.

The minor contribution of runoff erosion very close to divides for both F = 1 and F = 500 suggests that the neglect of variable source areas for runoff implicit in the use of (14) may not greatly affect landscape form.

The topographies produced with F = 1 (Figure 4) and F = 500 (Figure 6) are similar in broad pattern and drainage density (they start from the same initial conditions), but differ in details of morphology and pattern of branching. In the case of F = 1, low-order tributaries are relatively short compared with higher-order streams (low exterior-interior link length ratio), whereas the F = 500 channel system has nearly equal interior and exterior link lengths. In the latter

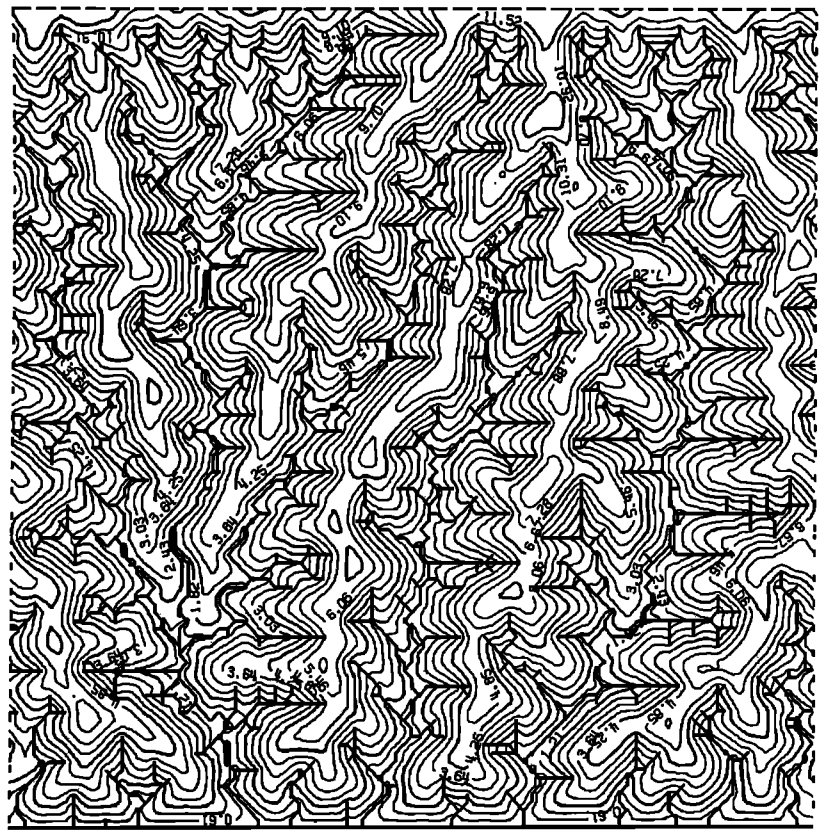

Figure 6. Steady state topography produced with $F = 500$ and no critical shear stress.

case, division of the landscape into low-order networks is more complete, and flow indirectness (average flow path lengths divided by straight-line distance to the basin mouth) is higher than for $F = 1$. In the case of $F = 500$, transitions from convex divides to channeled low-order streams is abrupt, whereas for $F = 1$, broad hollows occupy a comparatively larger proportion of the landscape. These morphological differences largely result from the more concave channel profile for the case of $F = 1$ than for $F = 500$ (see below).

Critical shear stress for fluvial erosion. Including a critical shear stress for fluvial erosion (τ_c in (16)) produces a very sharp transition between slopes and divides lacking any fluvial erosion and the channel network (Figure 7). The imposition of a critical shear stress lowers the drainage density and produces strongly convex slope profiles. Owing to the absence of fluvial erosion, the actual divergence on slopes near divides equals the theoretical divergence for erosion solely by diffusive mass wasting.

Although the critical shear stress is included to represent the flow conditions necessary to induce entrainment, it might also be used in an ad hoc manner to represent landscapes with permeable regolith in which runoff erosion on upper slopes is negligible and fluvial erosion first occurs in hollows from partial contributing area runoff.

Threshold mass wasting. If a critical threshold slope is assumed in mass wasting ($K_f > 0$ in (6)) and if creep moment is restricted (small K_s), then the rapid increase in mass wasting rates with slope gradient near the threshold means that the downslope increase in volume of mass-wasting debris in steady state topography can be accommodated by very slight changes in gradient. Slope profiles are therefore nearly linear, and divides are narrow and sharp (Figure 8). Such topography is common in subalpine areas with abundant frost-weathered coarse debris that undergoes appreciable movement only when gradients approach the angle of repose [*Carson and Petley*, 1970; *Carson*, 1971]. *Howard* [1994] argues that badlands in Mancos Shale near the Henry Mountains, Utah, which have nearly linear profiles and very narrow divides (Figure 9), are an example of mass wasting control under near-threshold conditions by sagging and small slumps.

Effect of Initial Conditions and Inheritance on Basin Form and Evolution

The initial topography has a strong influence upon the evolution of topography in the simulations, primarily through determining the overall layout of main channels and divides, less so in terms of details of individual slopes, and only modestly in terms of influence on averaged morphometric properties such as drainage density, hypsometric integral, and moments of slope gradient or divergence. Many of the simulations started from an initially nearly flat topography with random fractal perturbations which are many times smaller than the relief of the steady state topography. The simulated landscapes in Figures 10a and 10b have identical erosional histories, and simulation constants are identical, but the initial random fractal topography is different. The arrangement of drainage basins and divides is dissimilar, but the average basin morphometry is alike.

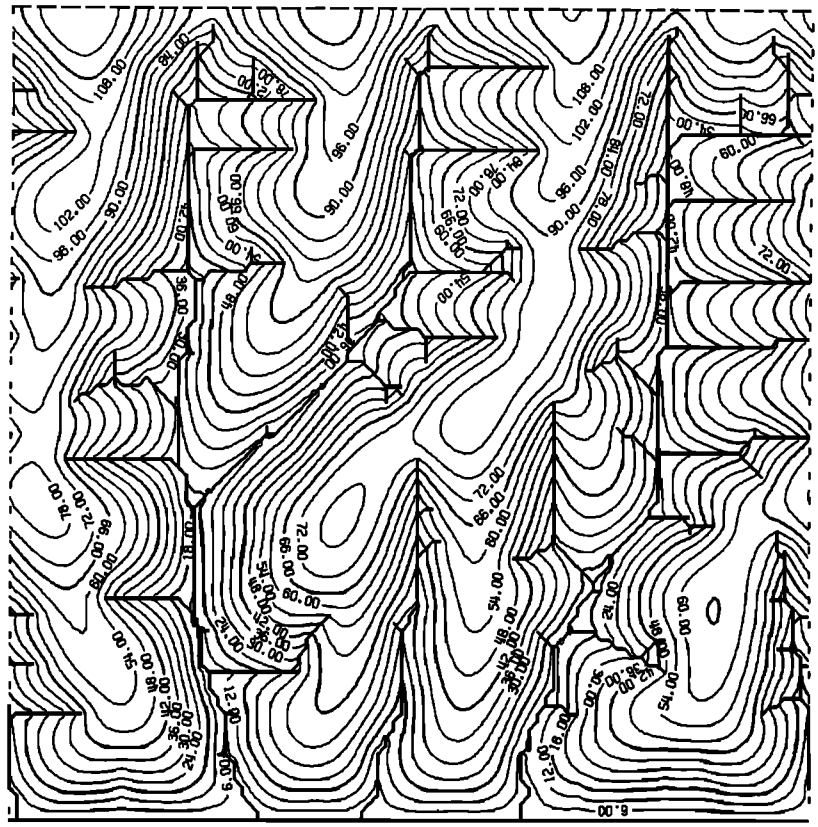

Figure 7. Steady state topography produced with $F = 500$ and a critical shear stress of 5.0.

Thus identical model parameters, spatial boundary conditions, and downcutting histories produces very different steady state drainage basins depending on initial conditions, and these differences can persist indefinitely. This means that a very wide range of possible steady state solutions to the equations governing basin evolution exist (e.g., (38)); there are, however, a presumably much larger set of topographic forms that are not steady state solutions.

Differences in initial conditions strongly influence transient behavior during early stages of dissection, and some systematic influences can persist even as steady state topography is approached. Figures 11a and 11c compare the early stages of evolution for different initial conditions, assuming that base level starts to drop at a constant rate at the beginning of the simulation. The basin in Figure 11a started from a nearly horizontal surface with very low relief fractal topography (the eventual steady state topography is shown in Figure 10a). Because of the low relief and therefore sluggish drainage, erosion progresses headward as a wave of dissection, similar to patterns observed in natural terrace and emergent lake bed erosion [*Carter and Chorley*, 1961; *Bryan et al.*, 1987; *Campbell*, 1989]. The pattern of headward extension is governed by the subtle fractal topography drainage divides on the upland. If the original topography is a nearly planar, but appreciably sloping surface (with slight superimposed fractal variation) dipping toward the base level edge (Figure 11b), the steeper gradients allow more rapid and more general dissection of the surface (Figure 11c), much as occurs in the dissection of natural alluvial fans. This dependence of dissection pattern upon initial surface slope was discussed by *Zernitz* [1932] and demonstrated in model erosion experiments by *Phillips* [1987]. The influence of the initial slope persists even into the steady state topography (compare Figures 10a and 11d). Basins produced by initially flat, fractal topography are irregular and wandering on the broad scale (although not at the scale of first- and second-order basins). By contrast, those resulting from dissection of a sloping surface are strongly aligned down the direction of the original slope and elongate. Therefore it is likely that natural drainage basins may retain in the broad arrangement of drainage channels and divides influences from very long ago.

Effect of Differences in Downstream Basin Concavity

In steady state simulations the downstream channel profile is a simple power function of drainage area. Using (16) and (21), setting $\partial z/\partial t$ to a constant erosion rate $-E$, and assuming that the contribution of eroded regolith per unit length of stream channel, $\partial z/\partial t|_m$, is a spatially uniform constant E_s:

$$S = K_u A^u, \tag{39a}$$

where

$$K_u = (E_c/K_t + \tau_c)/K_z, \tag{39b}$$

$$u = -0.6e(1 - b)/0.7, \tag{39c}$$

$$E_c = (E/\beta - E_s)/(F\xi) \tag{39d}$$

In the general case, K_u is a function of drainage area due to the terms β and ξ in (39d). If the regolith is much more erodible than the bedrock ($F \gg 1$), then $E_c \simeq E$ and K_u is

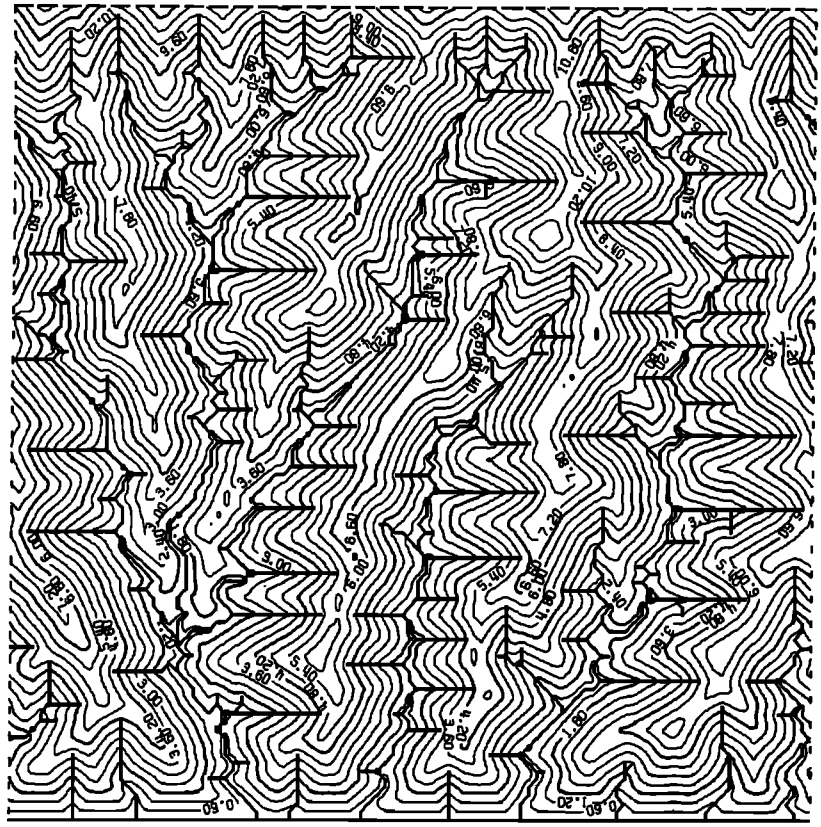

Figure 8. Steady state topography for simulation with a critical slope gradient ($K_f > 0$) in (6).

areally constant. If the assumed value of u is only slightly less than zero (Figure 12a with $u = -0.15$) then channel gradients decrease very slowly downstream. Simulated basins are long, narrow, and closely aligned along the regional topographic trend. The effect of initial conditions upon the drainage pattern is slight and indirect. Although the simulation model restricts junction angles to 45° increments, most junction angles are as small as is allowed (45°). If the assumed value of u is much less than zero (Figure 12b with $u = -1.0$), gradients decrease very rapidly downstream, and low-order basins are very compact and rounded, but high-order basins are wandering and irregular with drainage patterns strongly influenced by initial conditions. Junction angles tend to be larger than for the previous case. In the present model for bedrock erosion proportional to shear stress, an appropriate value for u is about -1.1 for $F = 1$ and -0.45 for $F = 500$. However, if bedrock erosion is more appropriately related to stream power as was assumed by *Seidl and Dietrich* [1992], the exponent u will be about -1.0 assuming $F = 500$ (Figure 12b). Although not simulated here, the circumstance where the major channels are sand bed alluvial results in downstream profiles with $u \sim -0.25$ [*Howard*, 1980; *Howard and Kerby*, 1983] and for coarse-bed alluvial $u \sim -0.6$ to -0.9 depending upon degree of downstream fining [*Hack*, 1957; *Pizzuto*, 1992].

Timescales of Approach to Steady State

All steady state simulations made under a variety of model parameters were examined to determine the length of time required to develop steady state topography from arbitrary, low relief initial conditions. Two criteria were utilized to define steady state: (1) no net change in average gradient from iteration to iteration and (2) approach to a constant, small number of local direction changes (a few local changes in flow direction persist into the steady state). So defined, steady state is reached after a cumulative lowering of base level that is approximately 3 times that of the final steady state relief. Slope profile simulations presented by *Ahnert* [1988] show a similar ratio between total erosion and relief at attainment of steady state.

Comparison With Optimal Drainage Basin Models

Several models of drainage basin development incorporating optimality criteria have been proposed over the years. *Howard* [1971a, 1990a] developed a "stream capture" model that starts from randomly generated drainage basins and modifies these by successively rearranging the drainage pattern such that streams follow the steepest available path downstream, assuming that gradients are related to drainage area via (39). *Howard* [1971a, 1972] showed that the stream capture algorithm minimizes both mean elevation and total stream power within drainage networks subject to (39) as a constraint. *Howard* [1971b, 1990a] also showed that (39) also implies optimal junction angles that are larger on the average as the absolute value of u becomes larger. The stream capture criterion and the junction angle model are self-consistent and also are consistent with a minimum power optimization criterion. Recently, *Rodriguez-Iturbe et al.* [1992], *Rigon et al.* [1993], and *Ijjasz-Vasquez et al.* [1993] have proposed a similar optimality criterion for basin morphology using (39) as the optimal relationship between gradient and drainage area. The optimal search algorithm of

Figure 9. Natural badland slopes in the Mancos shale badlands near Caineville, Utah. Note the nearly linear slope profiles and the very narrow divides.

Ijjasz-Vasquez et al. [1993] is essentially equivalent to the *Howard* [1971a] stream capture model.

By contrast, the present model is based upon mechanistic process laws not directly related to optimality criteria. However, the present model and the stream capture model can be compared in their predictions of steady state stream patterns. Starting conditions for a simulation with the present model were a gently sloping surface with superim-

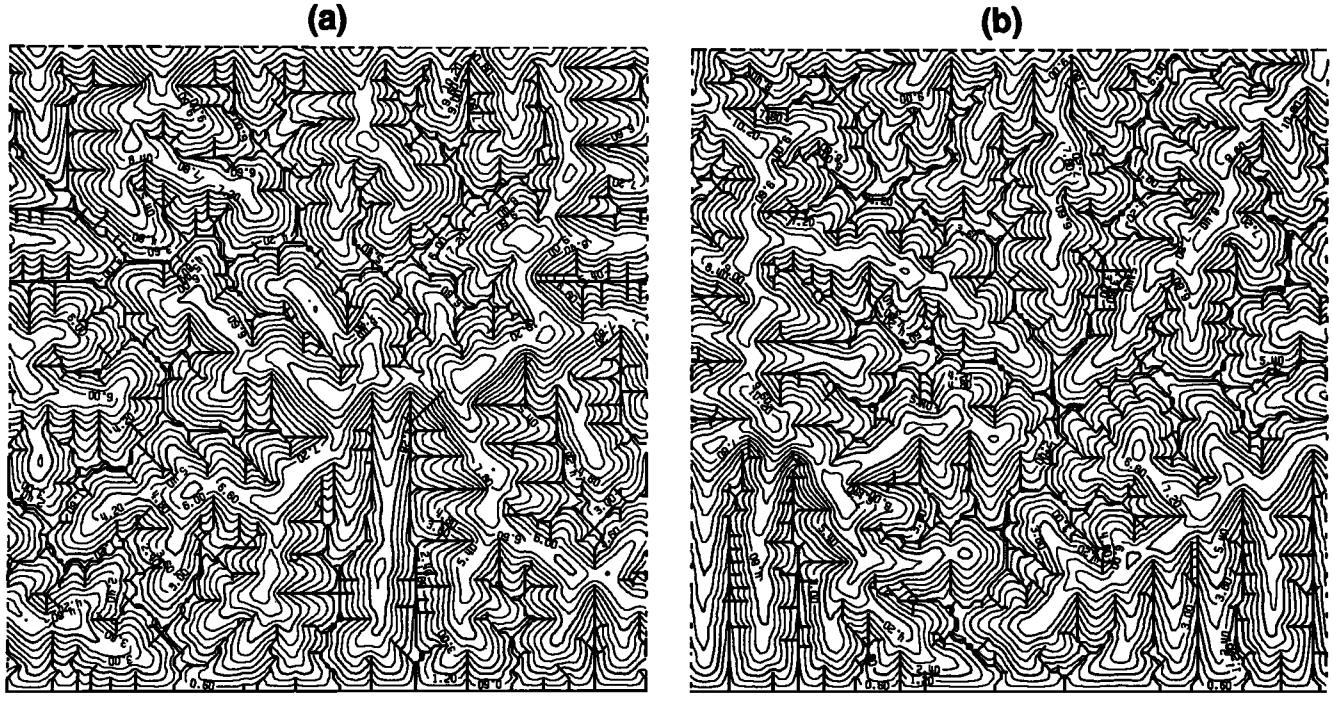

Figure 10. Two simulations of steady state topography for which initial conditions are different realizations of low-relief random fractal topography.

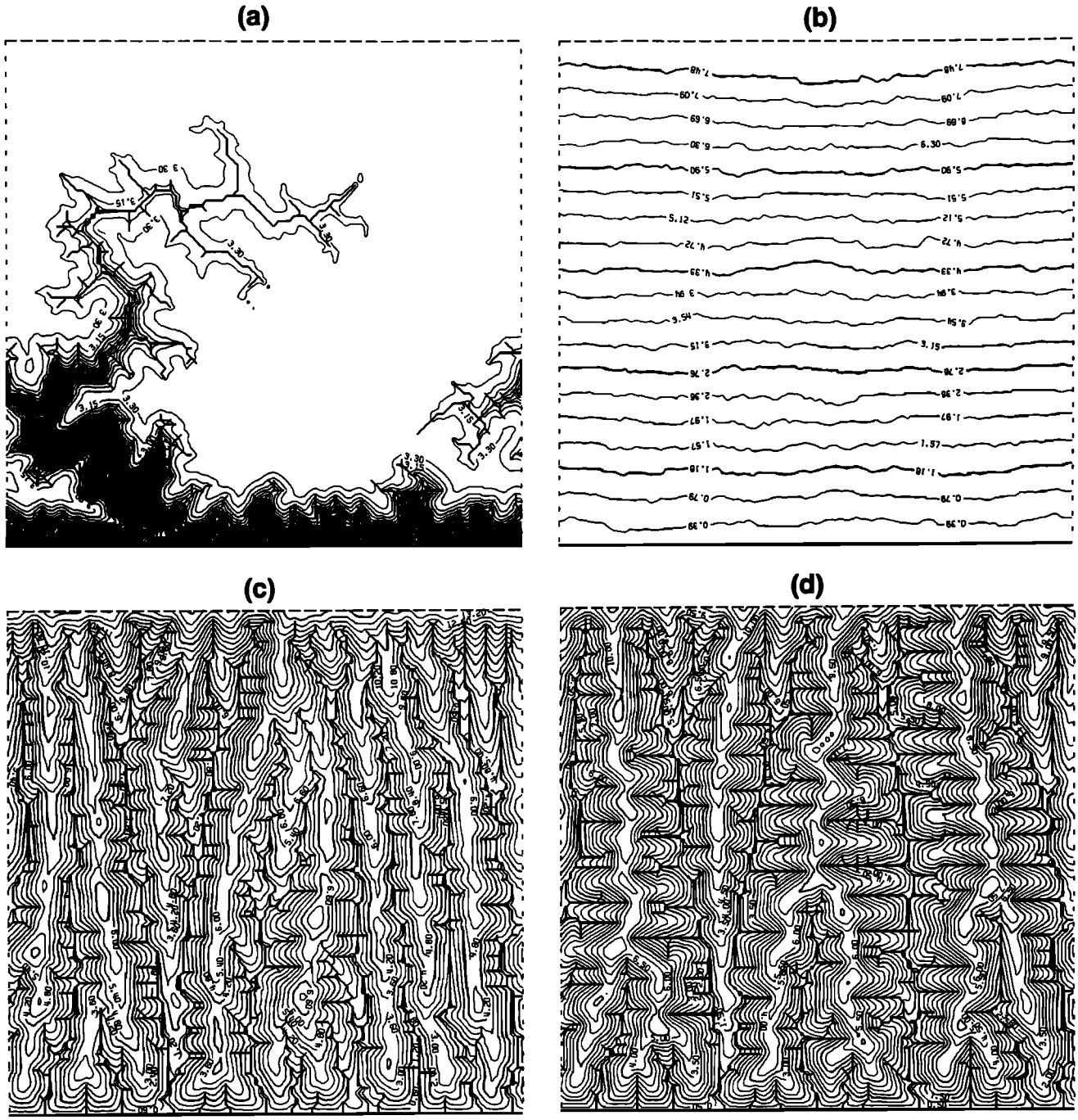

Figure 11. Simulations starting from different types of initial conditions. (a) Early stage of dissection of an initially very low relief random fractal topography. The final steady state landscape is shown in Figure 10a. (b) Initial conditions for the simulations shown in Figure 11c. This is a random fractal topography with a superimposed slope. (c) Early stage of dissection of the initial landscape shown in Figure 10b. Amount and rate of base level lowering equals that shown in Figure 11a. (d) The final steady state topography for the initial conditions shown in Figure 11b.

posed random fractal variations. Because the stream capture model requires an integrated drainage network as an initial condition, the drainage directions after 30 iterations of the present model with a constant rate of base level lowering were used to initiate the stream capture model (Figure 13a; stream pattern in Figure 13b). The basin after 500 iterations is shown in Figure 11c, and the steady state is shown in Figure 11d. The starting condition for capture is only slight dissection of the original surface, and stream gradients are far from attaining steady state adherence to (39). The stream patterns resulting from the steady state solution to the present model are shown in Figure 13c and may be compared with those produced by the stream capture model (Figure 13d). The stream capture model assumes that all locations on the matrix are drained by a stream, so that an assumed critical drainage area of five cells has been used to reduce the drainage density as plotted in Figure 13d to a value commensurate with that from the present model.

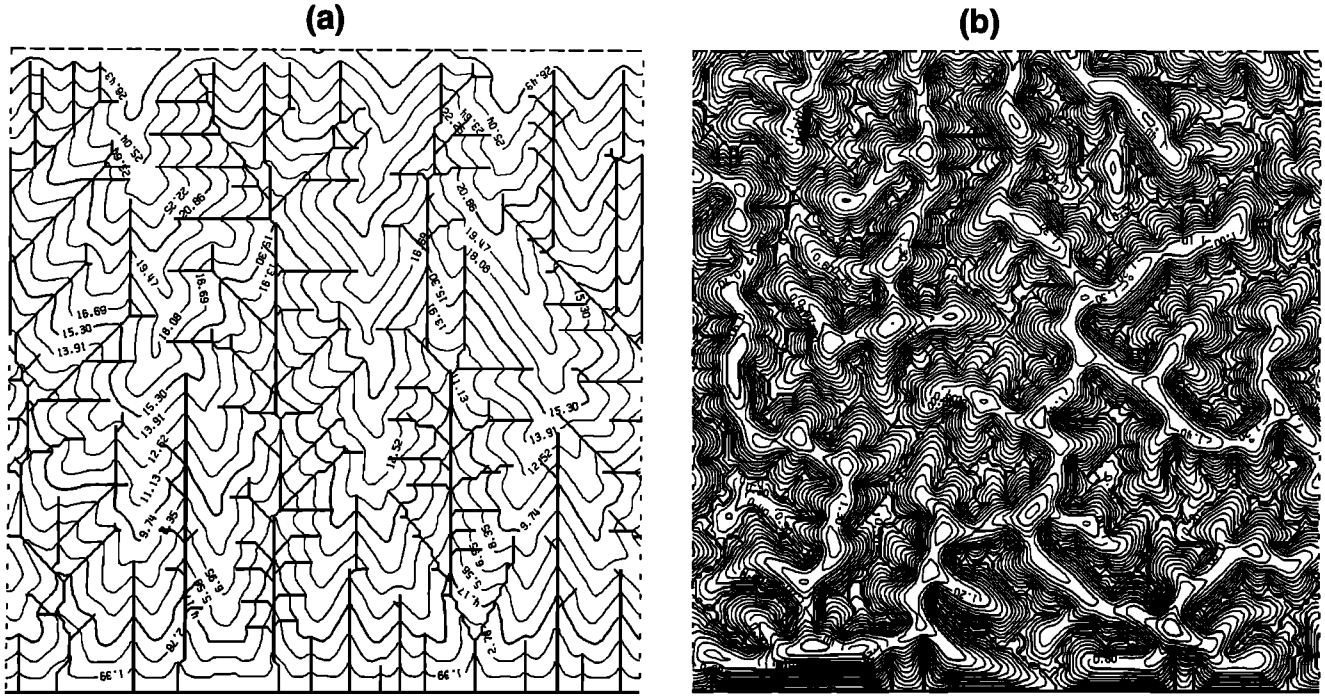

Figure 12. Effect of stream profile concavity on drainage basin morphology. (a) Steady state landscape in which downstream fluvial concavity u (39) equals -0.15. (b) Steady state landscape with $u = -1.0$.

The drainage patterns produced by both the present (Figure 13c) and stream capture models (Figure 13d) are similar in terms of the predicted location and shape of major basins and both are quite altered from the initial pattern (Figure 13b). Some discrepancies occur, as might be expected from exclusion of slope processes from the stream capture model. The similarity of predictions by the two models indicates that a closer comparison of their assumptions and processes of evolution is appropriate.

Two end-members of drainage rearrangement occur in the stream capture model. In downstream locations the classic case of capture of one stream by an adjacent one may occur. Similar captures can occur in the present model in the absence of intervening divides because water is assumed to follow the steepest path downhill. Most such changes in both models occur very early in basin evolution. In fact, by the time that 30 iterations had progressed in the present model (Figures 13a and 13b), most such captures had already occurred prior to creation of high divides. Only a few downstream captures occurred with either model during subsequent evolution, so that the high-order streams remained relatively fixed.

Drainage modification in the present model occurs primarily through the slow shifting of divides and the corresponding growth or abandonment of low-order streams. This occurs in response to asymmetry of relief on the two sides of a divide, much like the evolution of the Blue Ridge escarpment as discussed by *Hack* [1982]. Long, narrow basins in which the drainage area increases slowly downstream are at a competitive disadvantage to more compact basins, and they are often cannibalized by divide migration. This process is responsible for most of the changes in drainage pattern shown in Figure 13. The stream capture model also includes divide migration in an ad hoc manner in that headwater streams can be diverted to an adjacent drainage basin if the gradient from the head of the stream to the adjacent basin is steeper than the present downstream gradient.

Because streams are restricted to eight flow directions and must pass through matrix cell locations in the present model, the type of valley migration optimization proposed by *Howard* [1990a] cannot occur.

In conclusion, the present model and earlier optimality models produce similar predicted stream network morphology, and the physical processes incorporated in the present model can be viewed as an explanation for the success of the optimality models.

Definition of the Drainage Network and Area-Slope Relationships at Sources

The factors determining the location and density of valleys and stream channels in drainage basins is a perennial concern in geomorphology, with implications for understanding of drainage basin origin, scale and morphology, basin hydrology, and effects of natural and man-induced process changes, among other things. Some confusion has resulted from a failure to distinguish between the "channel" (or "stream") network, defined by channels with well-defined banks and sources [e.g., *Mark*, 1983; *Montgomery and Dietrich*, 1988, 1989, 1992; *Dietrich et al.*, 1992, 1993; *Dietrich and Dunne*, 1993] and the "valley" (or "drainage") network, which is defined on the basis of basin morphometry. These are, of course, related, in that stream channels occupy most drainage networks, but the channel network may expand or contract as a result of short-term climate or land use changes (for example, *Schumm* [1956a] and *Howard and Kerby* [1983] discuss seasonal cycles of rill growth due to summer rains and its infilling due to winter mass wasting, *Hack and Goodlett* [1957] and *Williams and Guy* [1973] outline extension of the channel network in the Appalachians due to scouring and avalanching and its gradual

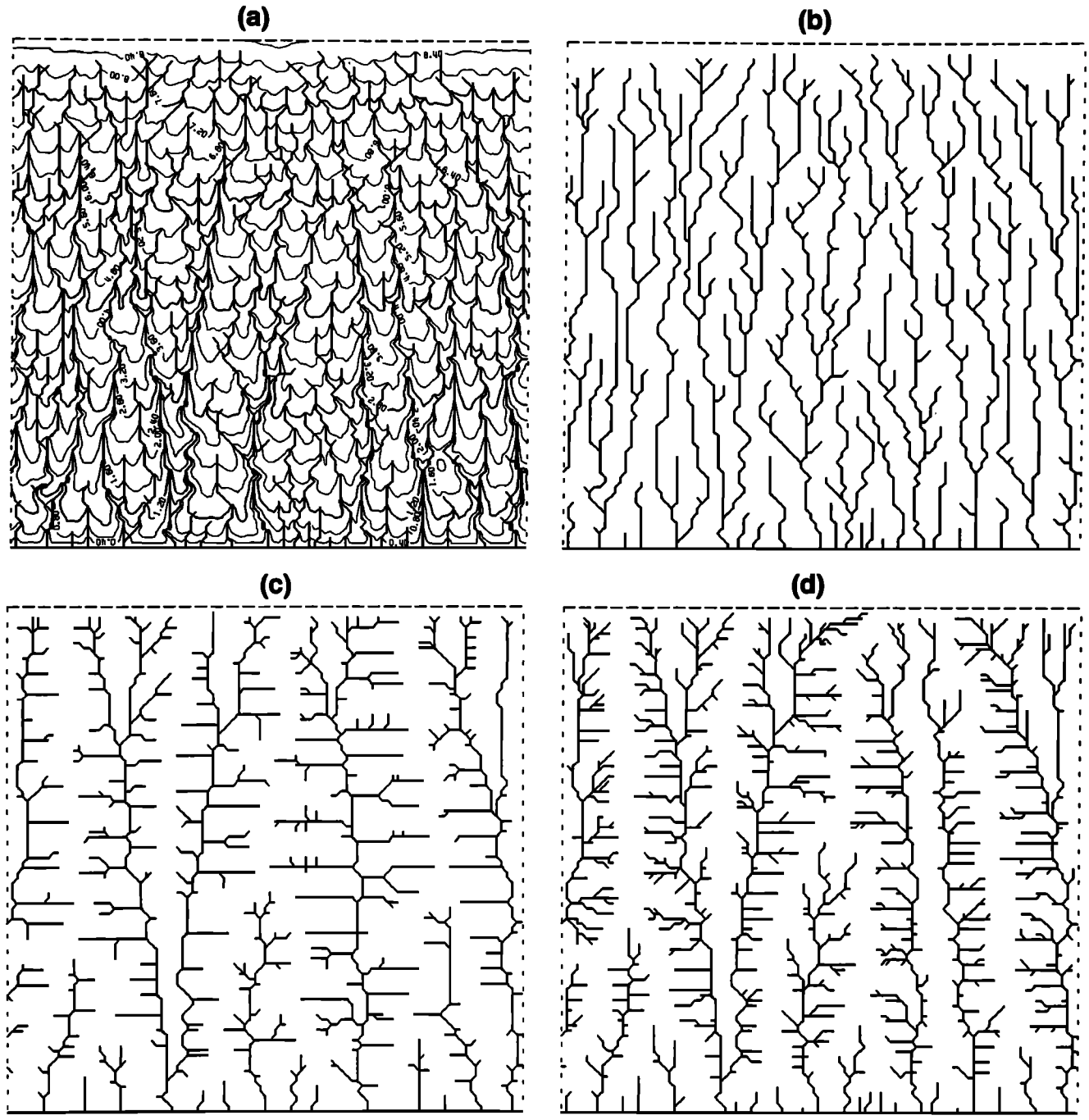

Figure 13. Comparison of drainage patterns produced by present model with *Howard*'s [1971, 1990a] stream capture model. (a) Very early stage of dissection of initial sloping, fractal landscape shown in Figure 11b. (b) Drainage pattern for landscape shown in Figure 13a, which serves as the initial conditions for the stream capture model (channels with drainage area less than five not shown). (c) Final steady state drainage network produced by present model (corresponds to landscape shown in Figure 11d). (d) Stream network produced by stream capture model starting from initial network shown in Figure 13b. Only channels with drainage area of five or greater are shown.

retreat between major storms, *Dietrich and Dunne* [1978] and *Dietrich et al.* [1986] show that headwater hollows are episodically flushed by landsliding, and there is a large literature on hillslope dissection by gullying due to climatic or land use changes). The factors determining the locations of channel heads can often be modeled by considering fluvial and/or landsliding processes singly or in combination (e.g., analyses of the threshold of runoff erosion and its implications to channel initiation [*Horton*, 1945; *Smith and Bretherton*, 1972; *Loewenherz*, 1991] and the recent application of process models to field location of channel heads by Dietrich and his colleagues [*Montgomery and Dietrich*, 1988, 1989, 1992; *Dietrich et al.*, 1992, 1993].

By contrast, valley networks result from the cumulative action of erosional processes over the longer timescales commensurate with the evolution of the large-scale topogra-

phy. A number of simulation models have illustrated the convexo-concave profile resulting from the downslope process transition from diffusional to concentrative [e.g., *Carson and Kirkby*, 1972; *Armstrong*, 1976; *Ahnert*, 1976, 1987a; *Hirano*, 1975, 1976; *Kirkby*, 1986, 1987; *Band*, 1985; *Willgoose et al.*, 1991a, b, c].

A network and its associated drainage density can be defined for either or both of the channel and valley system, but they are not equivalent. Field survey is generally necessary to define the channel network, although process modeling can help to produce predictive relationships based upon basin morphometry, as in the above-cited studies of Dietrich and colleagues. The valley network is morphometrically defined.

Although the model of *Willgoose et al.* [1991a, b, c] includes an activation threshold for the channel network, this is not a necessary feature for drainage basin development, as the present model illustrates. In the present model, concentrative as well as diffusional processes are assumed to occur within each landscape cell. However, there is a handover of process dominance in a narrow zone (Figure 5). In making the correspondence between the model and natural drainage basins, the channels on headwater convex and linear portions of the landscape presumably would be ephemeral, owing to the dominance of diffusional processes. In downstream valley bottom locations, the diffusional processes operate on slopes marginal to the stream within each cell (Figure 2), although overall erosion is dominated by fluvial erosion.

Thus in the present model neither a channel or valley network is specified a priori nor are channel heads defined by the governing equations (although in the case of a finite critical shear stress fluvial erosion starts abruptly at some distance from divides). Therefore an operational definition is required. One common approach has been to specify a critical support area [e.g., *O'Callaghan and Mark*, 1984; *Tarboton et al.*, 1991]. This approach is usable for drainage networks within areally uniform topography but is inappropriate for landforms with large areal variation in local relief [*Tribe*, 1992], such as the transient simulation shown in Figure 11a. The other major approach defines channels as all areas with concave upward topography [e.g., *Peuker and Douglas*, 1972; *Band*, 1986]. Surprisingly little work has been done to investigate other criteria, although *Mark* [1983] suggests contour curvature, and *Tribe* [1992] presents an algorithm that utilizes a threshold slope plus a V-shaped topography as criteria. Problems of distortions and noise (e.g., spurious sinks) in digital elevation data [e.g., *O'Callaghan and Mark*, 1984; *Band*, 1986; *Hutchinson*, 1989; *Moore et al.*, 1991; *Tribe*, 1992] may have contributed to the paucity of criteria. A variety of approaches to define the drainage network has been investigated during the present study. An ideal criterion should have the following properties: (1) it should be universally applicable, (2) the resulting network should not be strongly sensitive to modest variations in the defining parameter, (3) the definition should be related to natural process scales in the landscape, and (4) the drainage networks should correspond reasonably to those defined from maps by the usual contour crenulation method. Among the criteria investigated were critical and/or maximum values of slope gradient, gradient divergence, planform (contour) curvature, profile (downslope) curvature, and gradient divergence (a generalized curvature). These parameters were measured using 3 × 3 moving filters using the approach outlined by *Zevenbergen and Thorne* [1987] and *Moore et al.* [1991]. Among these, the gradient divergence normalized by mean gradient D was most successful in satisfying the above desiderata:

$$D = \nabla \cdot \mathbf{s}/\bar{s}, \tag{40}$$

where $\bar{s}$ is the average surface gradient within the simulation matrix. Matrix cells with D less than a critical value D_t are defined to have channels extending downgradient from the cell to the adjacent downstream cell. Figure 14 shows the drainage density that would be defined as a function of D_t for three steady state runs. These drainage densities are normalized such that a drainage density of unity corresponds to all matrix cells originating a channel. All of these curves exhibit a shoulder at which the rate change of drainage density with D_t is small. This shoulder generally lies between $-0.2 > D_t > -1.6$, and a value of -0.8 was selected for portrayal of the stream networks in all simulations shown here.

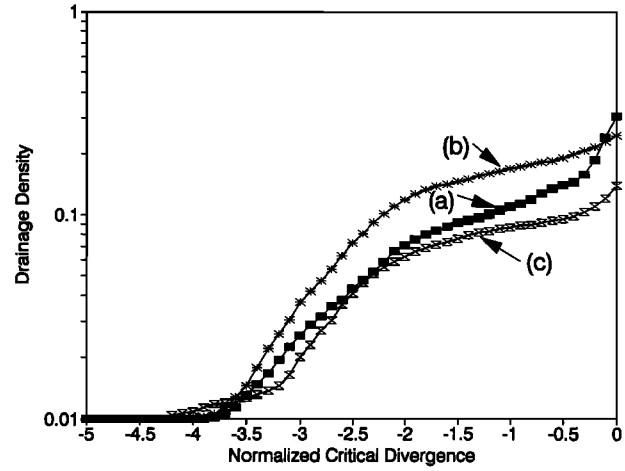

Figure 14. Drainage density resulting from assumption of various values of normalized critical divergence D_t, for (a) landscape shown in Figure 4, (b) landscape shown in Figure 6, and (c) landscape shown in Figure 7. Drainage networks shown in Figures 4, 6, and 7 correspond to $D_t = -0.8$.

This criterion delineates a drainage network that is very similar to that that would be drawn by hand using the contour crenulation method. It also performs well in landscapes with strong areal variation in relief, such as the transient dissection of an initially nearly planar surface shown in Figure 11a, in that stream channels are not defined on the flat upland. Furthermore, the use of gradient divergence as a criterion has a strong relationship to the process model assumptions, in that for almost all simulations mass wasting depends linearly upon gradient divergence, such that portions of the landscape dominated by mass wasting are characterized by positive D, whereas fluvial incision creates linear depressions with negative D.

The assumption of a critical D_t defining valley heads produces a relationship between contributing area and slope gradient at first-order valley heads similar to that observed by *Montgomery and Dietrich* [1988, 1989, 1992] for heads of channel networks. Plots of gradient-area values at drainage basin sources are presented in Figure 15 together with observed channel heads in a natural drainage basin. The

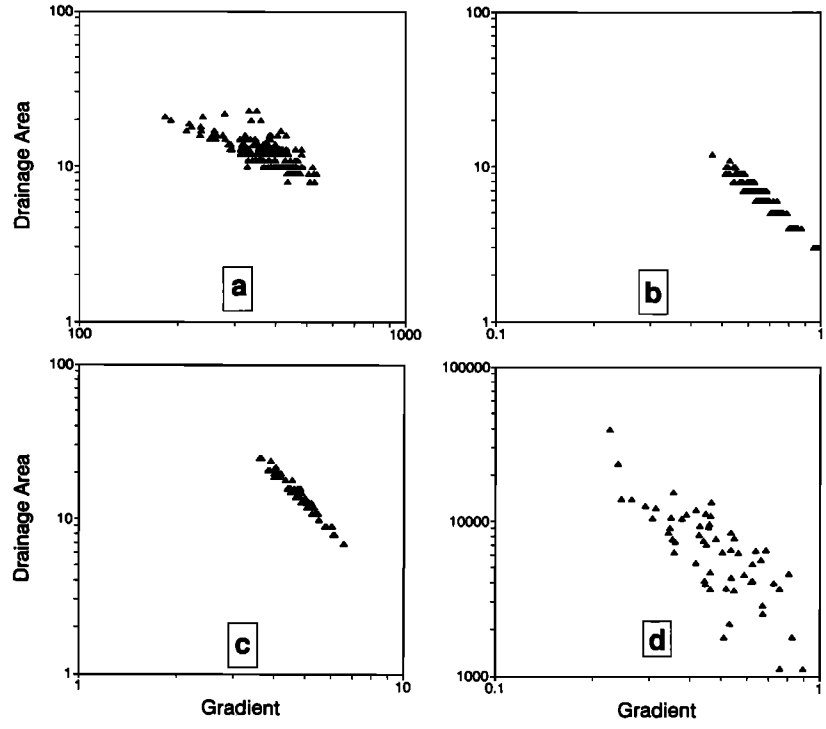

Figure 15. Relationship between drainage area and local gradient at sources (heads of first-order valleys) for simulated drainage basins compared with an area-gradient relationship for channel heads in a natural landscape, for (a) landscape shown in Figure 4, (b) landscape shown in Figure 6, and (c) landscape shown in Figure 7, and (d) channel head gradient-drainage area relationship for Tennessee Valley, California (data from *Montgomery and Dietrich* [1989]; drainage area is given in square meters).

slope of the drainage area-gradient relationship in these plots is determined largely by the stream channel profile concavity (Figure 5 and (39)). More importantly, the steady state "solutions" to first-order basin morphology in the present model permit a fairly wide range of gradients and source areas at valley heads having the same value of D in (40), presumably because of constraints introduced through competition for drainage area between adjacent basins.

Dietrich et al. [1992, 1993] propose models for a variety of mechanisms that may define stream heads, including critical thresholds for fluvial erosion, landslides, and regolith saturation. In the present model, only runs with a critical threshold shear stress for fluvial erosion (Figure 15c) have an intrinsic process change at drainage heads. In all other runs there is a gradual handover downslope between mass wasting and channel erosion processes. However, this handover is sufficiently abrupt that drainage network heads are well defined.

Is There a Characteristic Basin Form?

Willgoose [1994] shows that drainage basins formed by combined action of diffusive mass wasting and capacity alluvial sediment transport evolve toward a characteristic limiting basin morphology as relief declines. This limiting morphology is temporally constant when elevations are normalized by dividing by overall basin relief. This implies a pattern of basin evolution when base level is fixed in which slope and channel gradients proportionally decline, similar to that postulated for late stages of basin evolution by *Davis* [1932].

By contrast, if headwater channels are nonalluvial, there is no characteristic form. Figure 16 shows the subsequent evolution of the steady state basin topography in Figure 6 under conditions where the lower matrix edge (base level) is suddenly constrained to remain at a fixed level, and Figure 17 shows the decrease in the dimensionless hypsometric integral from the initial steady state to that of the topography in Figure 16. Slopes and headwater channels continue to erode at rates and with gradients little changed from the steady state values until elevations are reduced to very close to the now fixed base level, at which time gradients rapidly decline. Note that all channels in this simulation are specified to remain nonalluvial. This abrupt transition occurs first near the fixed base level and propagates headward. Thus base level control in headwater areas is indirect and slow to be manifested. The pattern of slope evolution in this case is more nearly consonant with models of parallel slope retreat [e.g., *Bryan*, 1940; *Penck*, 1953; *King*, 1953].

Mixed Alluvial and Nonalluvial Channels

A few simulations have been conducted in which both nonalluvial and alluvial channels are permitted. The simulation rules for transitions between the two types of channels have been discussed above. In general, alluvial channels occur in downstream areas where gradients decline to the point where supplied bed load sediment equals transport capacity. Two cases have been simulated: the development of an alluvial fan at a faulted mountain front and the gradual development of an alluvial pediment graded to a fixed base level.

The alluvial fan simulation is illustrated in Figure 18. Initial topography is a very slight slope toward the lower

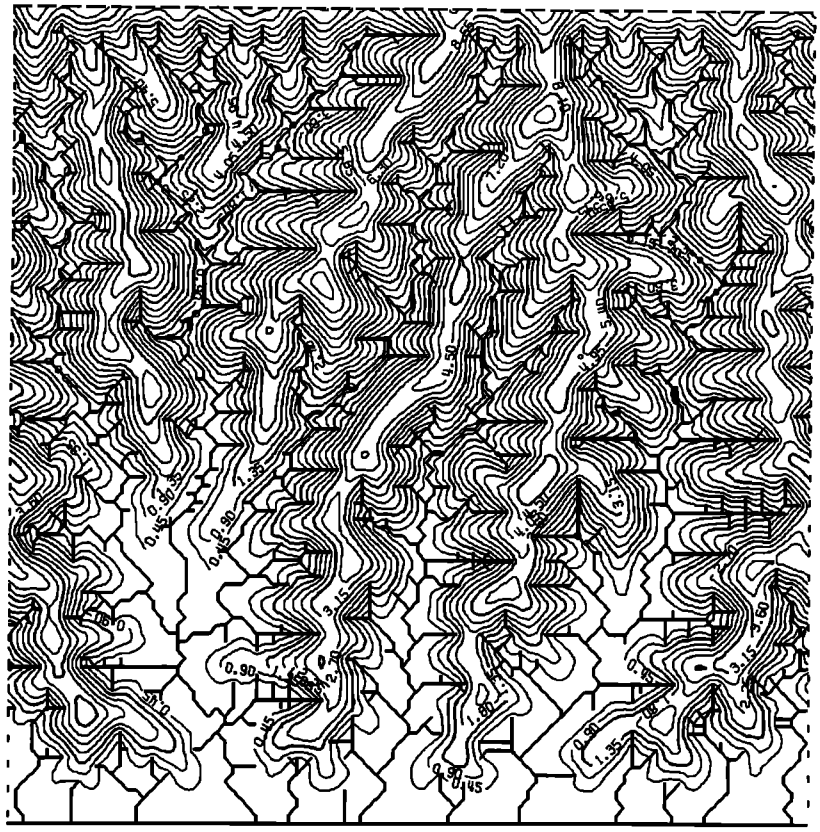

Figure 16. Landscape resulting from further erosion of initially steady state landscape shown in Figure 6 after base level becomes fixed.

edge interrupted by a steep scarp. Erosion of the scarp face is accompanied by fan deposition beyond the scarp base. All eroded regolith and bedrock is assumed to be of bed material size and to be deposited in the prograding fan. During each iteration the sediment and streamflow debauching from the scarp wall and the eroding canyons is routed downstream and deposited using the scheme presented in (30–36). Flow and sediment from each of the eroding channels follows a single course through the fan during each iteration, but owing to sediment deposition causing aggradation, alternate flow paths of steeper gradient across lower, older portions of the fan are utilized during subsequent iterations so that the fan form builds rather uniformly. The simulation illustrates the lateral interaction of fans of different sizes and the lower gradient of fans with larger contributing drainage areas (due to the greater sediment transporting capacity of larger discharges). Owing to the limitation of flow to one of eight directions at each cell, the fan assumes a prismatic shape during its growth. Along each flat face the total path length to the edge of the fan is equal. More realistic simulation of fan development will require either relaxation of the directional constraints or making the deposition process more irregular by having change of flow path (avulsions) be more difficult and somewhat random, corresponding to development and eventual breaching of levees as occurs on natural fans.

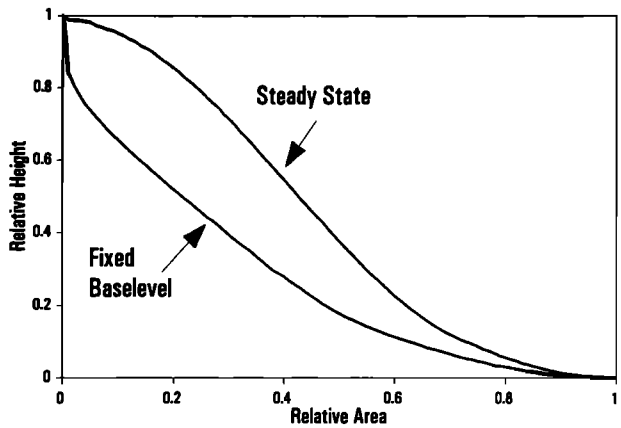

Figure 17. Dimensionless hypsometric curves of an initial steady state landscape (Figure 6) and the landscape resulting after base level becomes fixed (Figure 16).

The second simulation examines the development of an alluvial pediment graded to a fixed base level (Figures 19a and 19b). Initial conditions are a steady state topography resulting from a constant rate of base level lowering. The base level is then fixed, and as channel and slope gradients decline near the base level edge, a gradient is reached at which transporting capacity just equals sediment load supplied from upstream. As erosion progresses, the extent of alluvial channel expands, developing an alluvial expanse that is generally termed an alluvial surface or pediment, since the alluvial cover is thin. The alluvial channels slowly decline in gradient and elevation as a result of gradual decrease in sediment load from upstream as the headwaters are eroded. This pattern of slope replacement by expanding pediments has been well documented in badlands [*Johnson*, 1932;

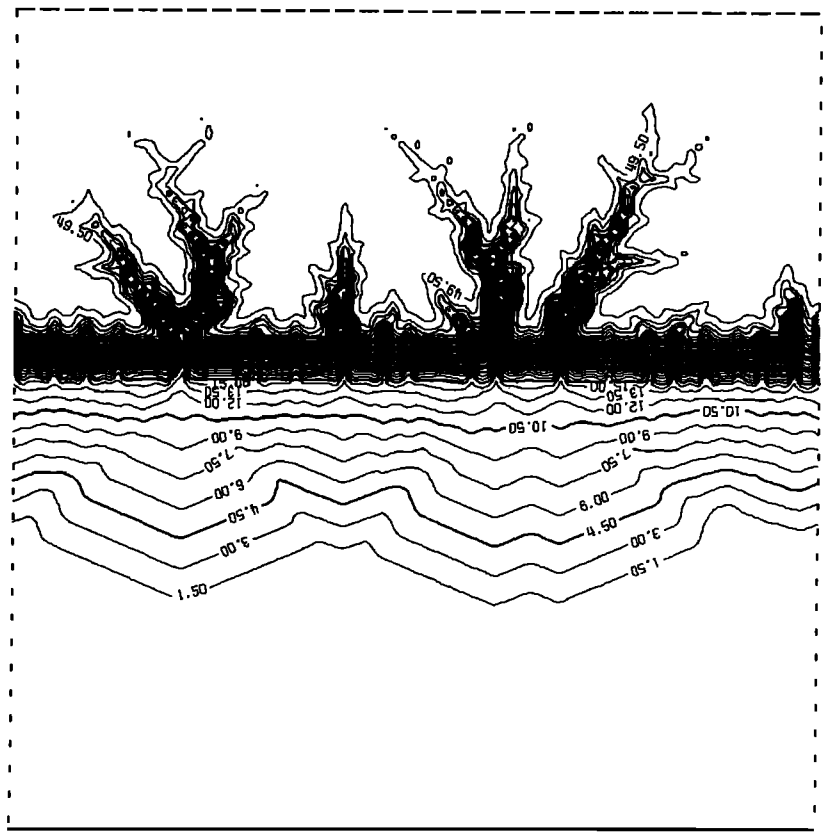

Figure 18. Simulated dissection of a steep scarp and deposition of eroded sediment in an alluvial fan complex. Base level at lower edge is fixed during simulation.

Bradley, 1940; *Smith*, 1958; *Schumm*, 1962]. An example occurs in Mancos Shale badlands (Figure 20) near the Henry Mountains, Utah, where creation of badlands by rapid downcutting of the main drainage channel (the Fremont River) has been followed by gradual retreat of the badlands and their replacement by an alluvial surface [*Howard*, 1970, 1994]. As is discussed above and is illustrated in Figure 19, the characteristic pattern of slope and channel evolution is nearly parallel retreat of slopes until remnant slopes between pediments are narrow and low, after which a slow rounding of slope profiles occurs [*Schumm*, 1956b; *Smith*, 1958].

A considerable speculative literature exists concerning the processes responsible for parallel slope retreat and replacement by encroaching pediments, both for badlands and for larger desert landscapes (see reviews by *Oberlander* [1989] and *Dohrenwend* [1994]). Most observers have postulated special processes operating at the abrupt junction between the retreating slopes and the advancing pediment, including lateral planation, erosion by spreading waters or emerging throughflow, and erosion due to hydraulic jumps. However, the process model presented here produces an abrupt, migrating pediment junction with no special processes other than the downslope increase in fluvial erosion potential due to greater runoff volume.

Fine-bed alluvial channels have a less convex profile ($u \sim -0.2$ in (39)) than nonalluvial channels ($u \sim -0.5$ to -1.1). As a result, a downstream transition from nonalluvial to alluvial can occur in steady state drainage basins for a range of values of constants in (10) and (28). Such landscapes are intermediate in appearance between those of Figure 4 or 6 and that shown in Figure 12a. The alluvial channels occur as a network only a single cell in width; this suggests that wide alluvial valleys common on some regions are produced either by valley widening due to meandering (not included in the model), or by a rate of base level lowering that is decreasing, static (Figure 19), or aggrading.

Conclusions

The present model has been argued to represent, in a general way, the interaction of processes that produce drainage basins. The model has been justified primarily by the assertions that (1) the mathematical formulation of processes is reasonable, (2) simulated steady state drainage basins resemble in a qualitative sense natural drainage basins in areas of uniform relief, and (3) simulations of transient landform development conform to our understanding of how natural basins evolve, including the initial dissection of flat or sloping surfaces, scarp dissection with fan deposition, and slope retreat with pediment development. Validation of models of drainage basin development is hampered by limited opportunity to compare predicted with observed landform evolution. One opportunity for direct validation is in badland landscapes, where process measurements are feasible and landform evolution may be rapid enough for quantitative comparisons. An example is in the Mancos Shale badlands near Hanskville, Utah [*Howard*, 1970, 1994], where badlands have been created by rapid downcutting of the master drainage since the end of the early Wisconsinian and where landform dating and process measurements are

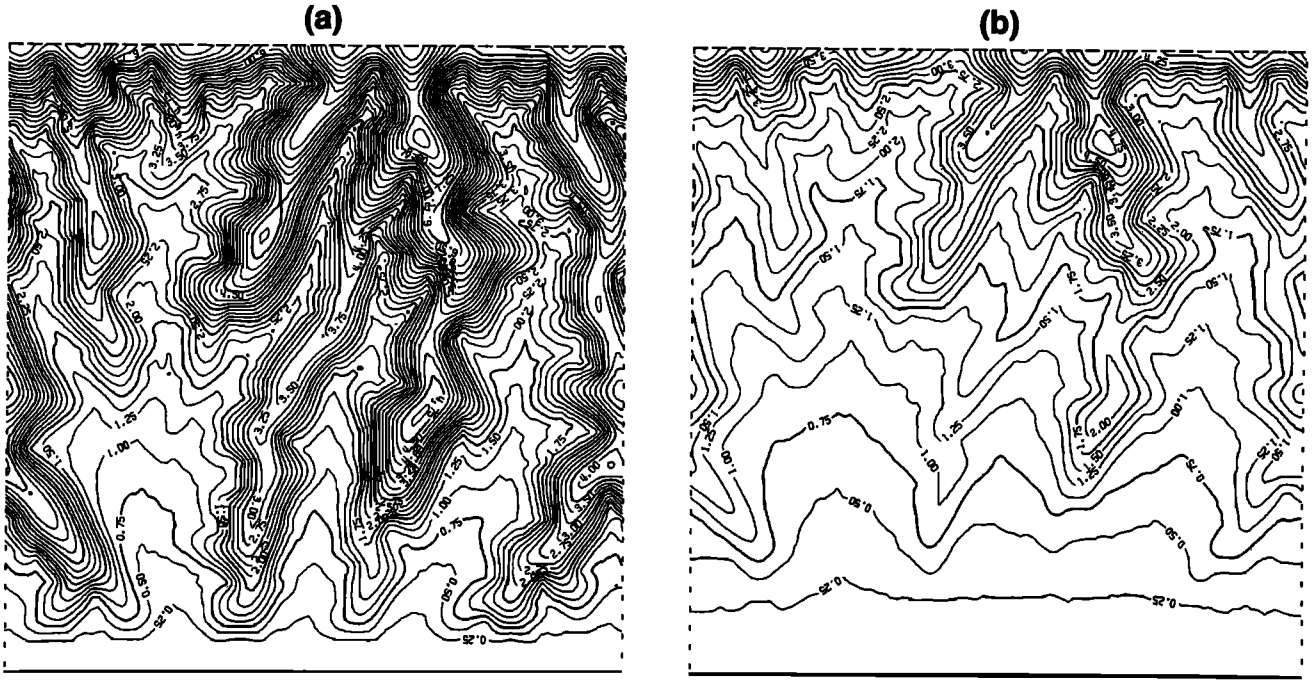

Figure 19. Development and headward prograding an alluvial surface during continued erosion of an initially steady state landscape. The base level at the bottom of the matrix is fixed at a constant elevation. Successive stages of alluvial surface growth showing nearly parallel retreat of upland slopes.

currently in progress (R. Anderson, personal communication, 1993). G. Willgoose (personal communication, 1993) is undertaking a validation effort for his drainage basin evolution model in application to erosion of a mining spoil heap. Another potential means of validation is to estimate the model parameters based upon field measurements and process modeling in areas of uniform relief coupled with simulation modeling to determine whether predicted steady state landforms resemble, in a statistical sense, the natural landscape. The field program and modeling efforts of *Dietrich et al.* [1992, 1993] may provide the parameterization for such a study. Neither of these techniques would be expected to reproduce a particular landscape (initial conditions are usually uncertain, and the details of resulting landscape depend sensitively upon the initial conditions). Therefore morphometric comparison of simulated and natural drainage basins will be necessary, but it will require development of new means of characterizing landform scale, length, orientation, and relief properties, since extant morphometric parameters only crudely characterize basin form. Possible approaches include statistical measures of hypsometry, gradients, junction angles, slope profiles, fractal properties, topology, and frequency domain analysis.

Although the model is poorly validated, a number of general observations about the model behavior probably also characterize general aspects of the evolution of natural landscapes with regolith-mantled slopes.

1. The model is deterministic, with randomness involved only in the development of the initial low-relief topography. The simulations show that even a small random component, as either initial or boundary conditions, is sufficient to provide the rich variation in landform texture that characterizes natural landscapes.

2. For a constant rate of base level lowering, a steady state topography eventually develops for any arbitrary initial topography. The steady state topographies produced from different initial conditions are different in detail but similar in general form (e.g., distributions of hillslope and channel gradients, drainage density, and slope profile characteristics).

3. Very simple additive models of erosional processes produce landforms with spatial properties similar to natural drainage basins. This suggests that despite the temporal and spatial complexity of erosional processes, long-term basin evolution can be approximated through the use of reasonably simple models.

4. As has been noted in field measurements of badland erosion, the relative importance of water erosion increases from the divide through the lower slopes to the streams.

5. The drainage pattern exhibits strong pattern optimization in the sense used by *Howard* [1990a], in that drainage paths from source to outlet are reasonably direct and the drainage density is nearly uniform.

This is not a model for all landscapes. Even assuming the model adequately represents the processes it addresses, there are many circumstances not covered, including (1) exposure and weathering of bedrock on slopes, (2) large volume changes upon weathering (e.g., karst), (3) erosion dominated by partial area runoff, including sapping processes, (4) the low-relief rock-mantled slopes discussed by *Abrahams et al.* [1994], (5) earth flows, energetic landslides, and debris avalanches, (6) transport in alluvial channels with appreciable downstream fining, (7) valley sidewall erosion by meandering, and (8) valley migration [*Howard*, 1990]. Some of these issues are addressed in the models of Ahnert and Kirkby cited earlier. Even in landscapes not well represented by the present process model, so long as there is a balance between a diffusive slope process and a concentra-

Figure 20. Badlands and alluvial surface in Mancos shale in the same general location shown in Figure 9. Badlands were created as a result of rapid lowering of the Fremont river (not shown), but recent stability of river elevation has permitted headward prograding of an alluvial surface accompanied by erosional retreat of the badlands. Compare with simulation shown in Figure 19.

tive channel process, most of the conclusions of this paper regarding general principles of landscape evolution would still be valid, particularly the inherent tendency to form slopes and integrated channels, the sensitivity to initial conditions, and the role of downstream channel concavity in determining basin shape.

In conclusion, the use of simulation models for addressing landform evolution in badlands (and drainage basins in general) has a bright future. The most important issues in use of such models are (1) developing appropriate process rate laws, (2) determining the boundary conditions (temporal and spatial) for the given situation, and (3) validation of the model through comparison of spatial variation in process rates or landform morphology between the model and the target natural landscape.

Acknowledgments. This research has been supported by a NASA planetary geology and geophysics grant (NAGW-1926). This work has benefited greatly from critical discussions with William Dietrich.

References

Abrahams, A. D., A. D. Howard, and A. J. Parsons, Rock-mantled slopes, in *Geomorphology of Desert Environments*, edited by A. D. Abrahams and A. J. Parsons, pp. 173–211, Chapman and Hall, London, 1994.

Ahnert, F., Brief description of a comprehensive three-dimensional process-response model of landform development, *Z. Geomorphol. Suppl.*, *25*, 29–49, 1976.

Ahnert, F., Some comments on the quantitative formulation of geomorphological processes in a theoretical model, *Earth Surf. Processes*, *2*, 191–202, 1977.

Ahnert, F., Approaches to dynamic equilibrium in theoretical simulations of slope development, *Earth Surf. Processes Landforms*, *12*, 3–15, 1987a.

Ahnert, F., Process-response models of denudation at different spatial scales, *Catena*, *10*, Suppl., 31–50, 1987b.

Ahnert, F., Modelling landform change, in *Modelling Geomorphological Processes*, edited by M. G. Anderson, pp. 375–400, John Wiley, New York, 1988.

Armstrong, A. C., Brief description of a comprehensive three-dimensional process response model of landform development, *Z. Geomorphol. Suppl.*, *25*, 20–28, 1976.

Band, L. E., Simulation of slope development and the magnitude and frequency of overland flow erosion in an abandoned hydraulic gold mine, in *Models in Geomorphology*, edited by M. J. Woldenberg, pp. 191–211, Allen and Unwin, Winchester, Mass., 1985.

Band, L. E., Topographic partition of watersheds with digital elevation models, *Water Resour. Res.*, *22*, 15–24, 1986.

Benda, L., The influence of debris flows on channels and valley floors in the Oregon Coast Range, U.S.A., *Earth Surf. Processes Landforms*, *15*, 457–466, 1990.

Blackwelder, E., The process of mountain sculpture by rolling debris, *J. Geomorphol.*, *4*, 324–328, 1942.

Bradley, W. H., Pediments and pedestals in miniature, *J. Geomorphol.*, *3*, 244–554, 1940.

Bryan, K., The retreat of slopes, *Ann. Assoc. Am. Geogr.*, *30*, 254–268, 1940.

Bryan, R. B., A. C. Imeson, and I. A. Campbell, Solute release and sediment entrainment on microcatchments in the Dinosaur Park badlands, Alberta, Canada, *J. Hydrol.*, *71*, 79–106, 1984.

Bryan, R. B., I. A. Campbell, and A. Yair, Postglacial geomorphic development of the Dinosaur Provincial Park badlands, Alberta, *Can. J. Earth Sci.*, *24*, 135–146, 1987.

Campbell, I. A., Badlands, and badland gullies, in *Arid Zone*

Geomorphology, edited by D. S. G. Thomas, pp. 159–193, Halstead, New York, 1989.
Carson, M. A., An application of the concept of threshold slopes to the Laramie Mountains, Wyoming, *Spec. Publ. Inst. Br. Geogr.*, *3*, 31–47, 1971.
Carson, M. A., and M. J. Kirkby, *Hillslope Form and Process*, Cambridge University Press, New York, 1972.
Carson, M. A., and D. J. Petley, The existence of threshold slopes in the denudation of the landscape, *Trans. Inst. Br. Geogr.*, *49*, 71–95, 1970.
Carter, C. S., and R. H. Chorley, Early slope development in an expanding stream system, *Geol. Mag.*, *98*, 117–130, 1961.
Davis, W. M., The convex profile of bad-land divides, *Science*, *20*, 245, 1892.
Dietrich, W. E., and T. Dunne, Sediment budget for a small catchment in mountainous terrain, *Z. Geomorphol., Suppl.*, *29*, 191–206, 1978.
Dietrich, W. E., and T. Dunne, The channel head, in *Channel Networks Hydrology*, edited by K. Beven and M. J. Kirkby, pp. 175–219, John Wiley, New York, 1993.
Dietrich, W. E., C. J. Wilson, and S. L. Reneau, Hollows colluvium and landslides in a soil-mantled landscape, in *Hillslope Processes*, edited by A. D. Abrahams, pp. 361–388, Allen and Unwin, Winchester, Mass., 1986.
Dietrich, W. E., C. J. Wilson, J. McKean, and R. Bauer, Erosion thresholds and land surface morphology, *Geology*, *20*, 675–679, 1992.
Dietrich, W. E., C. J. Wilson, D. R. Montgomery, and J. McKean, Analysis of erosion thresholds, channel networks, and landscape morphology using a digital terrain model, *J. Geol.*, *101*, 259–278, 1993.
Dohrenwend, J. C., Pediments in arid environments, in *Geomorphology of Desert Environments*, edited by A. D. Abrahams and A. J. Parsons, pp. 321–353, Chapman and Hall, London, 1994.
Dunne, T., Formation and controls of channel networks, *Prog. Phys. Geogr.*, *4*, 211–239, 1980.
Dunne, T., and B. F. Aubrey, Evaluation of Horton's theory of sheetwash and rill erosion on the basis of field experiments, in *Hillslope Processes*, edited by A. D. Abrahams, pp. 31–53, Allen and Unwin, Winchester, Mass., 1986.
Dunne, T., and W. E. Dietrich, Experimental study of Horton overland flow on tropical hillslopes, 1, Soil conditions, infiltration and frequency of runoff, *Z. Geomorphol. Suppl.*, *35*, 60–80, 1980.
Flemings, P. B., and T. E. Jordan, A synthetic stratigraphic model of foreland basin development, *J. Geophys. Res.*, *94*, 3851–3866, 1989.
Foster, G. R., Process-based modelling of soil erosion by water on agricultural land, in *Soil Erosion on Agricultural Land*, edited by J. Boardman, I. D. L. Foster, and J. A. Dearing, pp. 429–445, John Wiley, New York, 1990.
Foster, G. R., and L. D. Meyer, A closed-form soil erosion equation for upland areas, in *Sedimentation (Einstein)*, edited by H. W. Shen, pp. 12-1–12-19, Colorado State University, Fort Collins, 1972.
Gerald, C. F., and P. O. Wheatley, *Applied Numerical Analysis*, Addison-Wesley, Reading, Mass., 1989.
Gerits, J., A. C. Imeson, J. M. Verstraten, and R. B. Bryan, Rill development and badland regolith properties, in *Rill Erosion*, edited by R. B. Bryan, *Catena*, *8*, Suppl., 141–160, 1987.
Gilbert, G. K., The convexity of hilltops, *J. Geol.*, *17*, 344–351, 1909.
Hack, J. T., Studies of longitudinal stream profiles in Virginia and Maryland, *U.S. Geol. Surv. Prof. Pap.*, *294-B*, 97 pp., 1957.
Hack, J. T., Physiographic divisions and differential uplift in the Piedmont and Blue Ridge, *U.S. Geol. Surv. Prof. Pap.*, *1265*, 1982.
Hack, J. T., and J. C. Goodlett, Geomorphology and forest ecology of a mountain region in the central Appalachians, *U.S. Geol. Surv. Prof. Pap.*, *347*, 66 pp., 1960.
Hirano, M., Simulation of developmental process of interfluvial slopes with reference to graded form, *J. Geol.*, *83*, 113–123, 1975.
Hirano, M., Mathematical model and the concept of equilibrium in connection with slope shear ratio, *Z. Geomorphol. Suppl.*, *25*, 50–71, 1976.
Hodges, W. K., and R. B. Bryan, The influence of material behavior on runoff initiation in the Dinosaur Badlands, Canada, in *Badland Geomorphology and Piping*, edited by R. Bryan and A. Yair, pp. 13–46, Geo Books, Norwich, England, 1982.
Horton, R. E., Erosional development of streams and their drainage basins: Hydrophysical approach to quantitative morphology, *Geol. Soc. Am. Bull.*, *56*, 275–370, 1945.
Howard, A. D., A study of process and history in desert landforms near the Henry Mountains, Utah, Ph.D. dissertation, 198 pp., Johns Hopkins Univ., Baltimore, Md., 1970.
Howard, A. D., Simulation model of stream capture, *Geol. Soc. Am. Bull.*, *82*, 1355–1376, 1971a.
Howard, A. D., Optimal angles of stream junction: Geometric, stability to capture and minimum power criteria, *Water Resour. Res.*, *7*, 863–873, 1971b.
Howard, A. D., Problems in interpretation of simulation models of geologic processes, in *Quantitative Geomorphology: Some Aspects and Applications*, edited by M. Morisawa, pp. 61–86, Publications in Geomorphology, Binghamton, N. Y., 1972.
Howard, A. D., Thresholds in river regime, in *Thresholds in Geomorphology*, edited by D. R. Coates and J. D. Vitek, pp. 227–258, Allen and Unwin, Winchester, Mass., 1980.
Howard, A. D., Theoretical model of optimal drainage networks, *Water Resour. Res.*, *26*, 2107–2117, 1990a.
Howard, A. D., Preliminary model of processes forming spur-and-gully terrain, *NASA Tech. Memo.*, *TM 4210*, 355–357, 1990b.
Howard, A. D., Badlands, in *Geomorphology of Desert Environments*, edited by A. D. Abrahams and A. J. Parsons, pp. 213–242, Chapman and Hall, London, 1994.
Howard, A. D., and G. Kerby, Channel changes in badlands, *Geol. Soc. Am. Bull.*, *94*, 739–752, 1983.
Howard, A. D., and M. J. Selby, Rockslopes, in *Geomorphology of Desert Environments*, edited by A. D. Abrahams and A. J. Parsons, pp. 123–172, Chapman and Hall, London, 1994.
Hutchinson, M. F., A new procedure for gridding elevation and stream line data with automatic removal of spurious pits, *J. Hydrol.*, *106*, 211–232, 1989.
Ijjasz-Vasquez, E. J., R. L. Bras, I. Rodriguez-Iturbe, R. Rigon, and A. Rinaldo, Are river basins optimal channel networks?, *Adv. Water Resour.*, *16*, 69–79, 1993.
Imeson, A. C., and J. M. Verstraten, Rills on badland slopes: A physico-chemically controlled phenomenon, *Catena*, *12*, Suppl., 139–150, 1988.
Johnson, D., Miniature rock fans and pediments, *Science*, *76*, 546, 1932.
King, L. C., Canons of landscape evolution, *Geol. Soc. Am. Bull.*, *68*, 721–752, 1953.
Kirkby, M. J., Hillslope process-response models based on the continuity equation, *Spec. Publ. Inst. Br. Geogr.*, *3*, 15–30, 1971.
Kirkby, M. J., Soil development models as a component of slope models, *Earth Surf. Processes*, *2*, 203–230, 1976a.
Kirkby, M. J., Deterministic continuous slope models, *Z. Geomorphol. Suppl.*, *25*, 1–19, 1976b.
Kirkby, M. J., The stream head as a significant geomorphic threshold, in *Thresholds in Geomorphology*, edited by D. R. Coates and J. D. Vitek, pp. 53–73, Allen and Unwin, Winchester, Mass., 1980.
Kirkby, M. J., Modelling cliff development in South Wales: Savigear re-viewed, *Z. Geomorphol.*, *28*, 405–426, 1984.
Kirkby, M. J., The basis for soil profile modelling in a geomorphic context, *J. Soils Sci.*, *36*, 97–122, 1985a.
Kirkby, M. J., A model for the evolution of regolith-mantled slopes, in *Models in Geomorphology*, edited by M. J. Woldenberg, pp. 213–217, Allen and Unwin, Winchester, Mass., 1985b.
Kirkby, M. J., A two-dimensional simulation model for slope and stream evolution, in *Hillslope Processes*, pp. 203–222, edited by A. D. Abrahams, Allen and Unwin, Winchester, Mass., 1986.
Kirkby, M. J., Modelling some influences of soil erosion, landslides and valley gradient on drainage density and hollow development, *Catena*, *10*, Suppl., 1–14, 1987.
Lane, L. J., E. D. Shirley, and V. P. Singh, Modelling erosion on hillslopes, in *Modelling Geomorphological Systems*, edited by M. G. Anderson, pp. 287–308, John Wiley, New York, 1988.
Loewenherz, D. S., Stability and the initiation of channelized surface drainage: A reassessment of short wavelength limit, *J. Geophys. Res.*, *96*, 8453–8464, 1991.
Mark, D. M., Relations between field-surveyed channel networks

and map-based geomorphic measures, Inez, Kentucky, *Ann. Assoc. Am. Geogr.*, *73*, 358–372, 1983.
Matthes, F. E., Avalanche sculpture in the Sierra Nevada of California, *Bull. Int. Assoc. Sci. Hydrol.*, *23*, 631–637, 1938.
Meyer, L. D., Erosion processes and sediment properties for agricultural cropland, in *Hillslope Processes*, edited by A. D. Abrahams, pp. 55–76, Allen and Unwin, Winchester, Mass., 1986.
Montgomery, D. R., and W. E. Dietrich, Where do channels begin?, *Nature*, *336*, 232–234, 1988.
Montgomery, D. R., and W. E. Dietrich, Source areas, drainage density, and channel initiation, *Water Resour. Res.*, *25*, 1907–1918, 1989.
Montgomery, D. R., and W. E. Dietrich, Channel initiation and the problem of landscape scale, *Science*, *255*, 826–830, 1992.
Moore, I. D., R. B. Grayson, and A. R. Ladson, Digital terrain modelling: A review of hydrological, geomorphological, and biological applications, *Hydrol. Processes*, *5*, 3–30, 1991.
Moseley, M. P., Rainsplash and the convexity of badland divides, *Z. Geomorphol. Suppl.*, *18*, 10–25, 1973.
O'Callaghan, J. F., and D. M. Mark, Extraction of drainage networks from elevation data, *Comput. Vision Graphics Image Process.*, *28*, 323–344, 1984.
Oberlander, T. M., Slope and pediment systems, in *Arid Zone Geomorphology*, edited by D. S. G. Thomas, pp. 56–84, Halstead, New York, 1989.
Ostercamp, W. R., and J. R. Costa, Denudation rates in selected debris-flow basins, paper presented at Fourth Federal Interagency Sedimentation Conference, U.S. Interagency Advis. Comm. on Water Data, Las Vegas, Nev., 1986.
Paola, C., A simple basin-filling model for coarse-grained alluvial systems, in *Quantitative Dynamic Stratigraphy*, edited by T. A. Cross, pp. 363–374, Prentice-Hall, Englewood Cliffs, N. J., 1989.
Paola, C., P. L. Heller, and C. L. Angevine, The large-scale dynamics of grain-size sorting in alluvial basins, 1, Theory, *Basin Res.*, *4*, 73–90, 1992.
Penck, W., *Morphological Analysis of Land Forms*, Macmillan, New York, 1953.
Peucker, T. K., and D. H. Douglas, Detection of surface-specific points by local parallel-processing of discrete terrain elevation data, *Comput. Graphics Image Process.*, *4*, 375–387, 1975.
Phillips, L. F., Effect of regional slope on drainage networks, *Geology*, *15*, 813–816, 1987.
Pizzuto, J. E., The morphology of graded gravel rivers: A network perspective, *Geomorphology*, *5*, 457–474, 1992.
Rapp, A., Recent development of mountain slopes in Karkevagge and surroundings, northern Scandinavia, *Geogr. Ann.*, *42*, 73–200, 1960a.
Rapp, A., Talus slopes and mountain walls at Templefjorden, Spitzbergen, *Skr. Nor. Polarinst.*, *119*, 96 pp., 1960b.
Rigon, R., A. Rinaldo, I. Rodriguez-Iturbe, R. L. Bras, and E. Ijjasz-Vasquez, Optimal channel networks: A framework for the study of river basin morphology, *Water Resour. Res.*, *29*, 1635–1646, 1993.
Rivenaes, J. C., Application of a dual-lithology, depth-dependent diffusion equation in stratigraphic simulation, *Basin Res.*, *4*, 133–146, 1992.
Rodriguez-Iturbe, I., A. Rinaldo, R. Rigon, R. L. Bras, and E. Ijjasz-Vasquez, Energy dissipation, runoff production, and the three-dimensional structure of channel networks, *Water Resour. Res.*, *28*, 1095–1103, 1992.
Schumm, S. A., Evolution of drainage systems and slopes in badlands at Perth Amboy, New Jersey, *Geol. Soc. Am. Bull.*, *67*, 597–646, 1956a.
Schumm, S. A., The role of creep and rainwash on the retreat of badland slopes, *Am. J. Sci.*, *254*, 693–706, 1956b.
Schumm, S. A., Erosion on miniature pediments in Badlands National Monument, South Dakota, *Geol. Soc. Am. Bull.*, *73*, 719–724, 1962.
Seidl, M. A., and W. E. Dietrich, The problem of channel erosion into bedrock, *Catena*, *23*, Suppl., 101–124, 1992.
Smith, K. G., Erosional processes and landforms in Badlands National Monument, South Dakota, *Bull. Geol. Soc. Am.*, *69*, 975–1008, 1958.
Smith, T. R., and F. P. Bretherton, Stability and the conservation of mass in drainage basin evolution, *Water Resour. Res.*, *8*, 1506–1529, 1972.
Tarboton, D. G., R. L. Bras, and I. Rodriguez-Iturbe, On the extraction of channel networks from digital elevation data, *Hydrol. Processes*, *5*, 81–100, 1991.
Tarboton, D. G., R. L. Bras, and I. Rodriguez-Iturbe, A physical basis for drainage density, *Geomorphology*, *5*, 59–76, 1992.
Tribe, A., Problems in automated recognition of valley features from digital elevation models and a new method towards their resolution, *Earth Surf. Processes Landforms*, *17*, 437–454, 1992.
Willgoose, G., A physically based channel network and catchment evolution model, Ph.D. dissertation, Mass. Inst. of Technol., Cambridge, 1989.
Willgoose, G., A physical explanation for an observed area-slope-elevation relationship for catchments with declining relief, *Water Resour. Res.*, *30*(2), 151–159, 1994.
Willgoose, G., R. L. Bras, and I. Rodriguez-Iturbe, A coupled channel network growth and hillslope evolution model, 1, Theory, *Water Resour. Res.*, *27*, 1671–1684, 1991a.
Willgoose, G., R. L. Bras, and I. Rodriguez-Iturbe, A coupled channel network growth and hillslope evolution model, 2, Nondimensionalization and applications, *Water Resour. Res.*, *27*, 1685–1696, 1991b.
Willgoose, G., R. L. Bras, and I. Rodriguez-Iturbe, Results from a new model of river basin evolution, *Earth Surf. Processes Landforms*, *16*, 237–254, 1991c.
Willgoose, G., R. L. Bras, and I. Rodriguez-Iturbe, A physical explanation of an observed link area-slope relationship, *Water Resour. Res.*, *27*, 1697–1702, 1991d.
Willgoose, G., R. L. Bras, and I. Rodriguez-Iturbe, The relationship between catchment and hillslope properties: Explanation of a catchment evolution model, *Geomorphology*, *5*, 21–37, 1992.
Williams, G. P., and H. P. Guy, Erosional and depositional aspects of Hurricane Camille in Virginia, 1969, *U.S. Geol. Surv. Prof. Pap.*, *804*, 89 pp., 1973.
Zernitz, E. R., Drainage patterns and their significance, *J. Geol.*, *40*, 498–521, 1932.
Zevenbergen, L. W., and C. R. Thorne, Quantitative analysis of land surface topography, *Earth Surf. Processes Landforms*, *12*, 47–56, 1987.

A. D. Howard, Department of Environmental Sciences, Clark Hall, University of Virginia, Charlottesville, VA 22903. (e-mail: Internet ah6p@virginia.edu)

(Received September 29, 1993; revised February 28, 1994; accepted March 15, 1994.)